CRANFIELD UNIVERSITY

Jaime Pedret Pinilla

Study on the design of an attachment of a safety cage to a vehicle using LS-Dyna and test.

School of Engineering
Advanced Lightweight Structures and Impact

MSc Thesis
Academic Year: 2013 - 2014

Supervisor: Mr. Jason C. Brown
September 2014

CRANFIELD UNIVERSITY

School of Engineering
Advanced Lightweight Structures and Impact

MSc Thesis

Academic Year 2013 - 2014

Jaime Pedret Pinilla

Study on the design of an attachment of a safety cage to a vehicle using LS-Dyna and test.

Supervisor: Jason C. Brown
September 2014

This thesis is submitted in partial fulfilment of the requirements for the degree of Advanced Lightweight Structures and Impact MSc

ABSTRACT

This thesis includes an investigation into the mounting points of a Roll Cage on car frame using finite element methods.

On most of motorsports competitions vehicles or military purposes vehicles it is compulsory or highly recommended to fit a Roll Cage to the vehicle to prevent major damage of the car and protecting the occupants in the event of a roll-over accident.

A critical point in the design of a roll cage is the mounting points where the device is attached to the vehicle. A bad design of that part can result on a poor behaviour of the protection system on a crash event.

Beam element model is constructed from a wireframe geometry of a representative roll cage to quantify the forces that the attachments points receive on a typical FIA test. Then, FE models of different mountings configurations are created and parametrical study is performed in order to provide guidance on how to improve mountings performance.

Tests of two mountings specimens are carried to validate the FE models using a Rig created for this work.

Keywords:

Parametric Analysis, Design Guidance, FIA Regulations, Bolted, Reinforcement

ACKNOWLEDGEMENTS

I would like to give my most sincere gratitude to my thesis supervisor Mr. Jason C. Brown. He provided limitless effort on helping me throughout all my work, especially on testing procedures and was always kind to provide guidance when required.

Also, I truly appreciate the disposition to help and provide material and specimens of Safety Devices. Without their quick delivery of test specimens it would have not been possible to achieve the final objectives of this project. Many thanks to my industrial supervisor and contact with the company Mr. Chris Platt (Safety Devices' Design Engineer).

I would also like to thank Dr. Kevin Hughes for providing guidance on the FE modelling part of my work and allowing to perform the tests required on the department's lab.

Finally, I would like to my heartfelt gratitude to my family and the sacrifices they made for sending me abroad and giving me the chance to study in an internationally recognized institution. Many thanks to my friends and especially to those who made this year at Cranfield special.

TABLE OF CONTENTS

LIST OF FIGURES

LIST OF TABLES

LIST OF ABBREVIATIONS

SD	Safety Devices
FIA	Federation Internationale de l’Automobile
QMS	Quality Management System
SCTA	South California Timing Association
CDS	Cold Drawn Steel
SC	Safety Cage

1 INTRODUCTION

1.1 Aims of this work

Most of the accidents seen in common roads are normally rear or frontal impact of the vehicles. But another crash scenario is the rollover of the vehicle which is particularly violent in nature. Some studies state that a roll-over crash is far more likely to result in fatalities than a non-rollover crash. According to a study from the USA National Highway Traffic Safety Administration (NHTSA) in 2000 only 3 percent of all the passenger vehicles crashes where rollovers but that small percentage accounted for 20 percent of all the fatalities on the roads [1]

1-1. Rollover Road Accident

As the study states, the chances of a rollover crash scenario on the conventional roads are significantly low. Current cars are not as prepared for a rollover crash as they are for a frontal, lateral or rear impact. Figure 1-1 shows the aftermath of a rollover accident and how the roof of the vehicle has collapsed on the occupants.

Regarding other applications such as rally cars, expedition cars and military vehicles the conventional approach for the roof and car structure design is not valid given the higher possibility of a rollover accident compared to a conventional vehicle.

For this reason those special cars must be fitted with an extra structural feature on their body that prevents de collapse of the vehicle on a rollover called Safety cage or Roll Cage.

1-2. SD Roll cage protection. Mazda Championship MX5 [2]

A critical part of the roll cage design is the point where the structure is attached to the chassis of the vehicle. Therefore, the aim of this project is to understand the possible failure modes of that particular area and provide some guidance on how to improve the current mounting designs.

1.2 Safety Devices Ltd.

Safety Devices was founded in 1972 by former ‘Aley Bar’ designer Brian Wilkinson with Tony Willis and Collin Mynott. Around that time FIA decided to make roll cages mandatory and the homologated cage was born.

In 1976 Safety Devices started working with the British army. Their Land Rovers where fitted with external Roll Cages produced by the company.

1-3. SD Roll Over Protection. Land Rover Wolf [2]

By 1978 Safety Devices was the leading professional chassis preparation company employing approximately 70 people. Car preparation was performed in cooperation with leading car manufacturer companies including British Leyland, Ford, Opel, Vauxhall, Mitsubishi and Talbot. Safety Devices work consisted into taking a body from the production line and introduce modifications to the suspension, turret reinforcement, and of course, the design and installation of roll cages among other modifications.

After the recent success of the company Camel trophy moved to Safety Devices to fully equip their vehicles for their first expedition across the Amazonas basin. That relationship continued throughout the Camel Trophy era.

1-4. SD Roll Over protection. Camel Trophy Vehicle [2]

The company has constantly grown, in 1995 an automatic computer controlled robot was purchased by the company which automatically welded the roll cages together. In 2005, under the increasing pressure from the market for commercially competitive products the manufacturing operations were moved to Poland. After that manufacturing location change the 9001 ISO quality for the roll cages is still assured and in 2007 the QMS international certified SD with an ISO 9001 quality assured manufacturer.

Safety Devices was commissioned by SKODA to design and install a bespoke roll cage for a SKODA Octavia vRs. Lately that car became the world's fastest 2.0-litre supercharged production car when registered a SCTA sanctioned speed of 227.07 mph.

On 2012 the company celebrated the 40th anniversary since its creation.

2 CONTEXT TO THE PROJECT

2.1 Safety Cage Structure

A safety cage is a multi-tubular structure fitted close to the bodyshell and its main function is to reduce the deformation of the chassis in case of accident, particularly in a roll-over accident scenario. For a good Safety Cage design is highly recommended to comply with the FIA technical regulations or use them guidance for the design. In Safety devices, most commonly dimensions used for roll cages tubes are 44.45x2.64mm. It is also used tubes 44.45x2.03mm and 38.1x2.64mm for bracing.

2.2 Safety Cage Applications

The range of applications for a Safety Cage is very wide. In the particular case of Safety Devices Ltd. the products offered vary from a motorsport safety cage suitable for competition to products like a Roll Over Protection Safety (ROPS) cage suitable for military purposes in the event of roll over.

2.3 Extent of the project

This project is focused in the study on mountings of the Cage to the bodyshell of the vehicle. If an excellent safety cage in terms of rollover and crash protection is achieved but the mountings to the vehicle and the chassis itself is very poor, the structure will no accomplish its requirements.

3 OBJECTIVES and TASK LIST

3.1 Objectives

The objectives for this project are identified as the following

- Study of factors affecting stiffness and strength of a roll cage foot mounting using test and simulation.
- Parametric study or improvement of roll cage foot mounting.

3.2 Task list

To achieve those objectives, a series of task are planned:

1. Use LS-DYNA non linear FE software for collapse analysis.
2. Initial simplified full Rollcage FE model to find max. structural loads on mounting feet.
3. Experimental validation of baseline model
4. Compare collapse performance of alternative baseline foot designs.
5. Parametric modelling to assess possible foot and reinforcement improvements.
6. Conclusions: suggested design improvements.

4 BASELINE MODEL DESIGNS

Baseline model consist on four different mounting configurations based on Safety Devices suggestions. Main content of this work is to study the behaviour of the different suggested designs. All different designs present similarities but slight

differences exist between designs. On the following images a schematic representation of the mountings is presented.

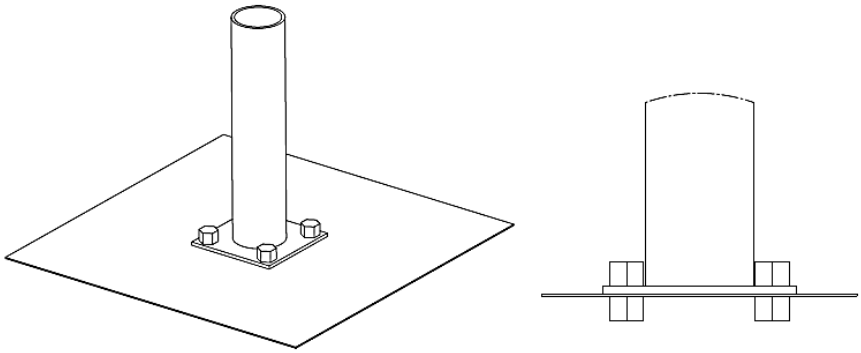

4-1. Configuration 1. Simply Bolted

A tube of standard SD Ltd. size is welded to a foot plate and plate is bolted to a 1mm plate representing the floor frame of the vehicle.

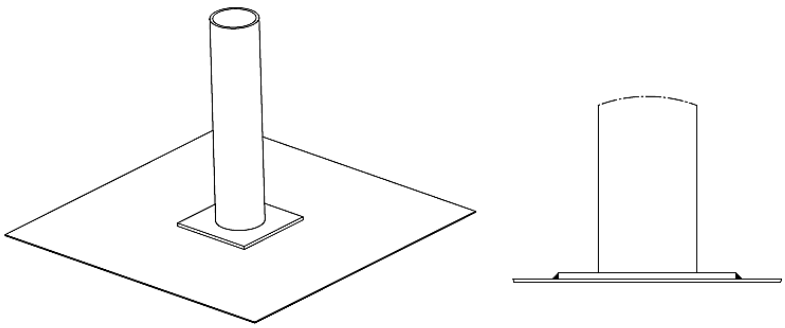

4-2 Configuration 2. Simply Welded

On this configuration, instead of bolting the foot plate to the floor, the edges are welded to the plate representing the floor of the vehicle. Both on C1 and C2 no reinforcement plate is used.

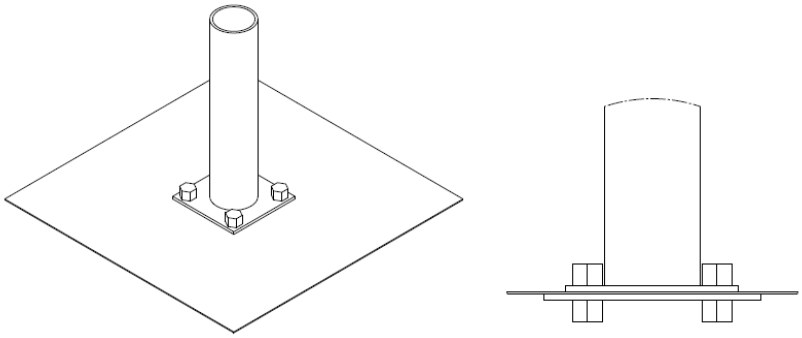

4-3 Configuration 3. Bolted

On the called bolted configuration, a similar construction as C1 is used. The main difference observable is that an additional reinforcement plate is placed underneath the floor plate and bolted together with the foot plate using the same bolts.

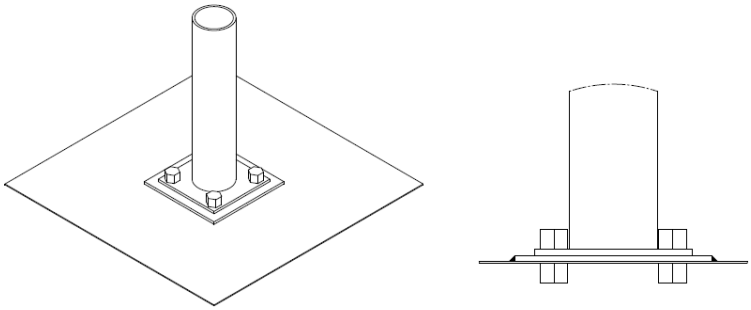

4-4 Configuration 4. Welded

Finally, on the last configuration a reinforcement plate is welded on top of the floor. Then foot plate with the tube is bolted above the reinforcement along with the floor.

Materials used for tube, reinforcement and foot plates is CDS 355N as indicated by the company. Floor plate is modelled using typical material properties for vehicle frame, mild steel 170MPa [3].

Further details regarding dimensions and materials are included in the appendix section A.

5 LITERATURE RESEARCH

For this project some previous research is performed. This research includes features like the recommended design of a roll cage by the FIA and the Rollcage test procedure.

More specifically, and as the mounting feet of the roll cage are bolted to the chassis, bolted connections behaviour is briefly revised.

Bending of thin walled circular tubes is checked as the model will include circular tubes and it is necessary to ensure that their behaviour is correct.

5.1 Roll Cage Design (FIA Technical Regulations) [4]

A roll cage is formed by some basic elements that are recommended to be included in all designs. Those elements are presented in the technical regulations of the Federation Internationale de l'Automobile (FIA). Whether the structure is used or not for FIA competitions is strongly recommended to use those regulations as guidelines for the design. Although only a part of the structure is the main study of this project it is important to know how the whole cage is designed.

According to art. 253 [4] on FIA regulations, the main elements are the following.

DEFINITIONS

Rollbar

Tubular frame forming a hoop with two mounting feet

Main Rollbar

Transverse and near vertical (max 10^{o} angle to the vertical) single piece tubular hoop located across the vehicle just behind the front seats (figure 5-2**¡Error! No se encuentra el origen de la referencia.**).

The tube axis must be within one single plane.

Front Rollbar

The geometry is similar to the main Rollbar's geometry but its shape follows the A pillars and screen top edge geometry.

Lateral Rollbar

Single piece tubular hoop on the sides of the roll cage, with two mounting feet each.

Lateral half-Rollbar

Identical to the lateral Rollbar but not containing the rear pillar on the structure.

Transverse member

Single pieced tube joining the lateral Rollbar and half-Rollbar members.

Diagonal member

Transverse tube between one top corner of the main Rollbar, or one of the ends of the transverse member in case of lateral Rollbar, and the lower mounting point on the opposite side of the Rollbar.

Can also be included between the upper point of the backstay and the lower mounting point of the other backstay.

Mounting foot

Plate welded to the end of the Rollbar tube that allows the connection between the roll cage and the body frame of the car. (This plate must be welded in addition to the bolts)

Reinforcement plate

Metal plate added between the mounting foot and the chassis of the car to provide stiffness to the floor structure and spread the loading onto the floor.

Gusset

Reinforcement for a junction made from a U shaped metal sheet. Thickness of the plate must not be less than 1 mm. figure 5-1

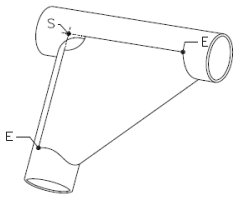

5-1. [4]

BASIC STRUCTURE

- Figure 5-2. 1 main Rollbar + 1 front Rollbar + 2 longitudinal members + 2 backstays + 6 mounting feet.
- Figure 5-3. 2 Lateral Rollbars + 2 transverse members + 2 backstays + 6 mounting feet.
- Figure 5-4. 1 main Rollbar + 2 lateral half-Rollbars + 1 transverse member + 2 backstays + 6 mounting feet.

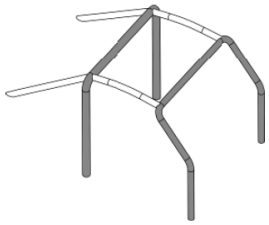

5-2. [4]

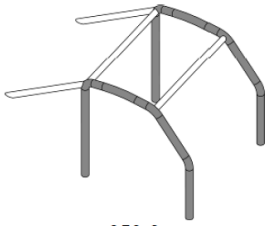

5-3. [4]

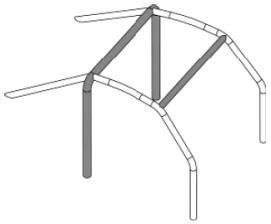

5-4. [4]

From those basic structures, some reinforce members must be also added to the structure.

COMPULSORY MEMBERS AND REINFORCEMENTS

Diagonal member

Structures must include a diagonal member of the figures (5-5, 5-6, 5-7 and 5-8). In case of the figure 5-7 the distance between the two members' mountings on the body shell must not be bigger than 300mm.

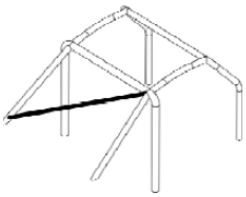

5-5. [4]

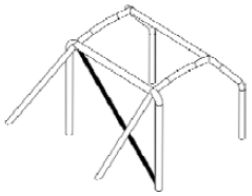

5-6. [4]

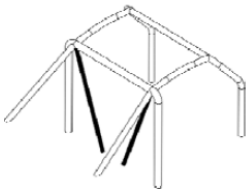

5-7. [4]

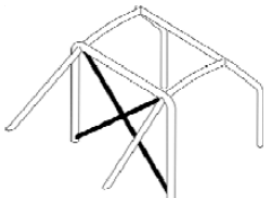

5-8. [4]

The reason for including those diagonal members is to triangulate the structure and avoid lateral crushing of the roll cage.

Doorbars

One or more longitudinal members must be added at each side of the structure according to figures 5-9, 5-10, 5-11 and 5-12. The design must be equal on both sides and combinations of configurations can be used.

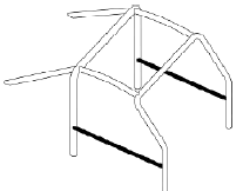

5-9. [4]

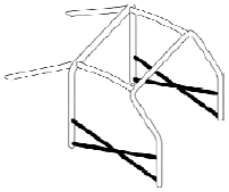

5-10. [4]

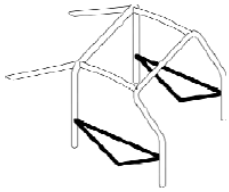

5-11. [4]

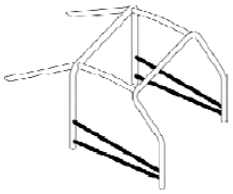

5-12. [4]

Roof reinforcement

The upper part of the roll cage must be designed according to the following figures.

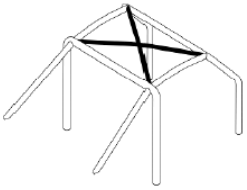

5-13. [4]

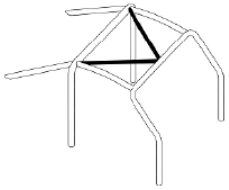

5-14. [4]

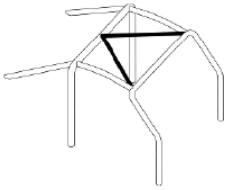

5-15. [4]

Windscreen pillar reinforcement

Finally, the last compulsory reinforcement member is the one fitted on each side of the front rollbar if dimension A is bigger than 200mm. Design shown on figure 5-16.

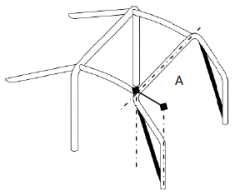

5-16. [4]

MOUNTING OF ROLL CAGES TO BODYSHELL/CHASSIS

Minimum mounting points:

- 1 for each pillar of the front rollbars
- 1 for each pillar of the lateral rollbars or lateral half-rollbars
- 1 for each pillar of the main rollbar
- 1 for each backstay

Mounting points of the front, main, lateral rollbars or lateral half-rollbars:

- Each mounting point must contain a reinforcement plate at least 3mm thick.
- Each mounting foot must be attached by at least three bolts on a steel reinforcement plate at least 3mm thick and of at least 120 cm^2 area which is welded to the bodyshell.
- Fixing bolts must have a minimum diameter of M8 and a minimum quality of 8.8 (ISO Standard)
- Fasteners must be self-locking or fitted with lock washers.
- The angle between 2 bolts (measured from the tube axis at the level of the mounting foot) must not be less than 60 degrees. (figure 5-17)

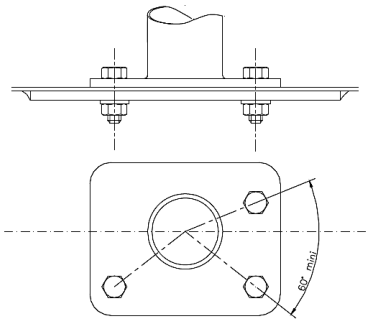

5-17. [4]

5.2 FIA Roll Cage Test

According to FIA homologation regulations three test load cases must be applied to the structure.

The approved FIA design is certified to withstand loads of 7.5w daN vertically on the main hoop and 3.5 daN on the front windscreen. [5]

The article also states that the manufacturer must demonstrate its ability to manufacture roll cages regarding the materials, welding methods and the quality standard procedures.

If previous requirements cannot be ensured by the manufacturer a test must be performed on the Rollcage. Following points are included in the test procedure:

1. RollCage
   The test must be performed on the complete Rollcage.
2. Test rig.
   The device must be capable of withstand the loads applied into the Rollcage
3. Mountings
   Mountings used to attach the car to the structure must be included in the test specimen.
4. Test
   A 7.5w daN force is applied with a stamp of a minimum area 500x200mm on the main roll bar.
5. Maximum deformation

The structure will pass the test if there is not a bigger displacement than 50mm at any point of the Rollcage.

5.3 Bolts Preload [6]

Bolted connections are present in the attachment between the roll cage structure and the chassis. To ensure that the connection will be tight during service it is necessary to apply a load in the fastener existing prior to the application of external loading. As a result of this preloading a contact force between the plates is obtained which may change when an external load is applied. Although modelling assessment of this phenomena is carried, it is not included on final FE models to keep computing time lower and simplify the model. On further studies bolts preload is recommended to be implemented.

Given a simple fastener in tension shown in the figure 5-18 below, B_0 represents the force of the bolt and C_i is the contact forces of the plates. If no external load is applied to the connection the force on the bolt and the contact force of the plates are equal [6].

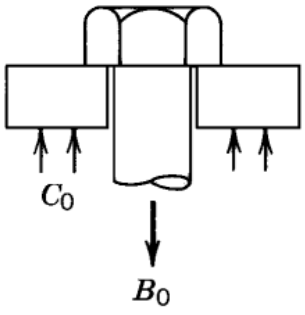

5-18. Bolted Connection [6]

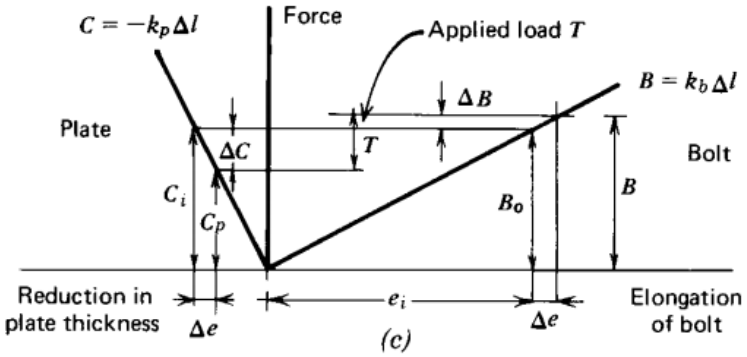

5-19. Force in Prestressed Fastener [6]

When an external load T is applied the fastener will elongate and the precompressed plates will expand. If the expansion suffered by the plates is lower than the initial precompression there will be some contact force remaining. With that, the equilibrium requirement for the connection states,

$$B = T + C_p$$

where B is the bolt force under the applied force T and C_p is the contact force remaining between the plates. Note that when external force T reduces the contact between plates to 0 and in consequence the plates separate, force B on the bolt equals to external force T. The following graph presents the bolt loading in function of the external applied force T.

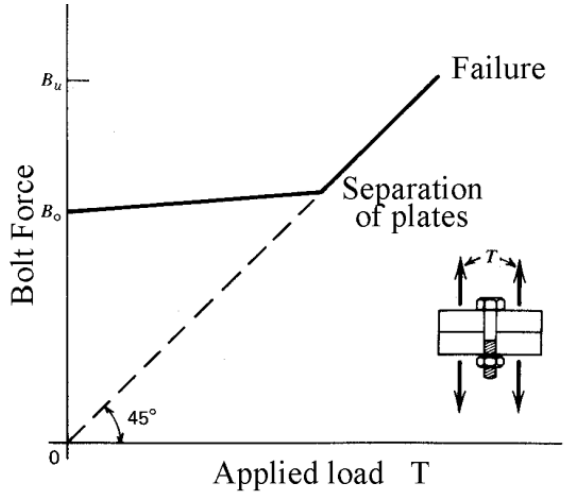

5-20. Bolt force vs applied load for preloaded bolted connection

Force B remains practically constant while applied load T increases. Typically at that section of the curve force B increases less than 10%. At the point where the plates separate and there is no contact force between them, the loading T acts only on the bolt and force B increases in the same amount as the external loading. If external force T increases after plates separation can lead to a bolt failure.

5.4 Failure of circular section tubes

In a structure like a safety cage containing tubes the failure will be caused by axial or torsional failure of individual tubes and more probably by bending.

The collapse mode of the tubes are completely different whether the tube is a thin-walled section or thick-walled. In the present work the tubes are assumed to be thin walled section as the tube diameters (D) of a roll cage are more than 10 times higher than the thickness of the wall (t).

5.4.1 Axial failure mechanism [13]

When submitted to compression a thin-walled tube can fail by Euler buckling or Crumpling. Buckling is likely to appear for long tubes with small section while for wide section tubes of small thickness, which is the case of the Rollcage tubes, the probable failure mode is Crumpling figure 5-21.

5-21. Square Section Tube Axial Failure

5.4.2 Bending failure mechanism [10]

Given a clamped beam subjected to a load at the other end the moment caused by the force will vary linearly along the length, being maximum at the clamped end (figure 5-22).

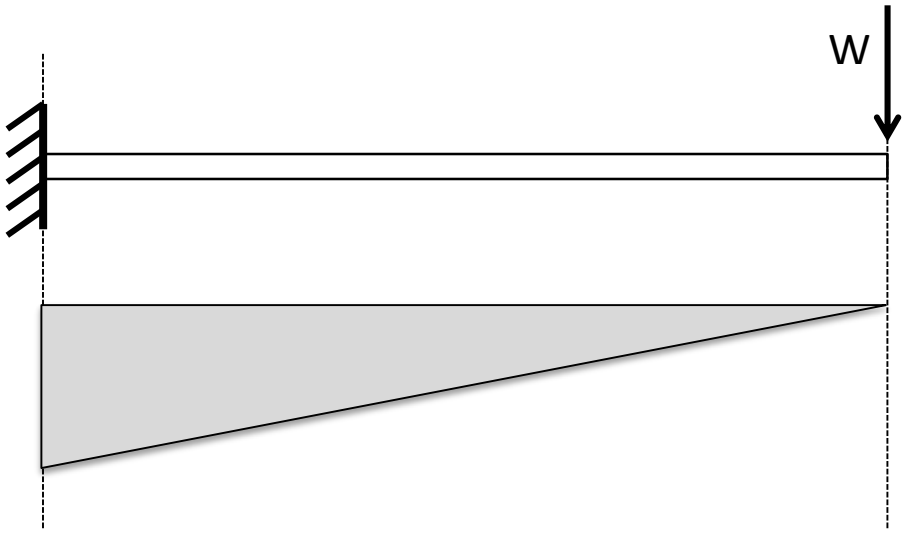

5-22. BMD Clamped Beam

The typical collapse mechanism for a thin walled section is the following:

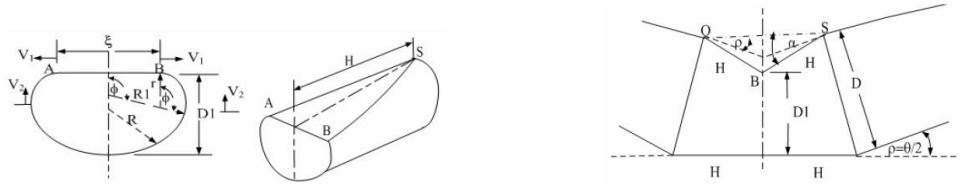

5-23. Platic Collapse of Thin-Walled Circular Tube Subjected to Bending

- When subjected to bending, hinge lines appear (AB) when the collapse force is reached.
- A flattening of the circular section of the tube is observed.

On a study performed by S.Poonaya [10] collapse mechanism of circular tubes is analysed. The study divides the collapse mechanism of a tube subjected to bending into three phases: elastic behaviour, ovalisation plateau and structural collapse.

In elastic phase, the moment is assumed to increase linearly up to a yield moment rotation. Linear moment-rotation characteristic curve is predicted using elementary theory of elasticity.

$$M_y = \frac{2\sigma_y I}{D_0};\ \theta_y = \frac{M_y L_0}{EI}$$

Where M_y is yield moment, L_0 is the pure moment length, E is the elastic modulus, I is the second moment of area, σ_y is the measured yield stress, θ_y is the yield rotation angle and D_0 is the outside diameter of the tube.
In ovalisation phase he initially circular cross section presents slight hardening due to the deformation. Ultimate moment resisted by the tube is equal to the following.

$$M_{ovalised} = S_{ovalised}\sigma_y$$

Where $S_{ovalised}$ is the plastic section modulus of an ovalised tube and σ_y is the measured yield stress of an ovalised tube.

In phase 3, structure starts to collapse resulting load carrying capacity decreases rapidly. Three resisting moment components corresponding each to a different crushing phenomena are used to obtain analytically third phase.

$M_1 = \left(\frac{\frac{-1}{4}.\frac{(-R+r)}{R}.M_0.\frac{\pi}{R}.t.\sqrt{2}.\phi}{\theta}\right)$ is moment component crushing of the ring.

$M_2 = \left(\frac{5.9.10^{-2}.\frac{(-R+r)^2}{R^2.H}..M_0.t.\phi^3}{\theta}\right)$ is moment component central hinge.

$M_3 = \left(\frac{\frac{1}{32}.\frac{\sqrt{2}}{R^2}(R-r).M_0.t.\phi}{\theta}\right)$ is moment component for oblique hinge.

Where R is tube's cross section radius, r is equal to 0.6R, θ is bending rotation, ϕ is mechanism angle defined using θ and $M_0=4\sigma_0R^2t$ is the fully plastic bending moment of the undeformed cross section.

Previous formulations are derived according to some assumptions.

1. Tube material is ductile, rigid-perfectly plastic, isentropic, homogeneous and material compatibility condition is maintained.
2. Tube circumference is inextensible.
3. Shear and twist deformation are neglected.
4. Collapse hinge mechanism deforms in a simplified manner.
5. All hinges are assumed straight.
6. Tube cross section radius (R) is the initial mean radius of the tube.
7. Tube does not elongate or contract in axial direction
8. Parameters H and r are constant during collapse.

Poonaya used testing to validate analytical formulation above with following results.

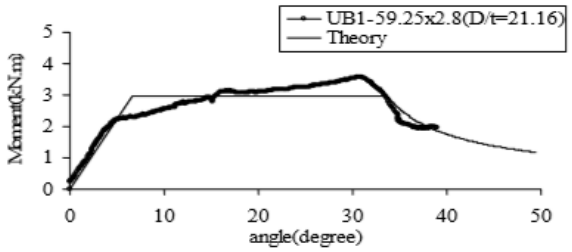

(a)UB1

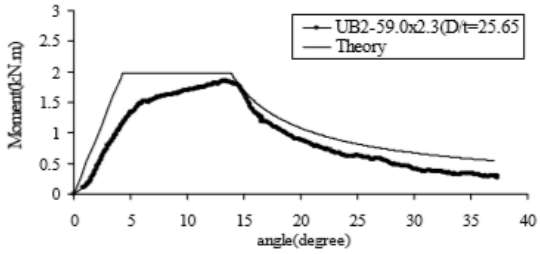

(b)UB2

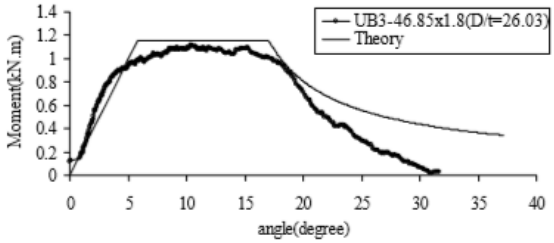

(c)UB3

5-24. S.Poonaya [10] Experimental vs. Analytical

S. Poonaya's study formulae is used on section 7.2.3 to validate circular tube's FE models needed for current work.

6 SOFTWARE BACKGROUND AND MODELLING FEATURES

6.1 LS-DYNA3D

LS-DYNA is a general purpose, finite element software package developed by the Livermore Software Technology Corporation [11]. Code's origins lie in highly nonlinear, transient dynamic finite element analysis using explicit time integration Nonlinear calculations at least one of the following complications: changing boundary conditions (contacts), large deformations or nonlinear materials that don't exhibit elastic behaviour.

Transient dynamic involves analysing high speed events where inertial forces are important. This capability is important for example to simulate automotive crash.

It also includes other interesting features such as thermal analysis, fluid analysis, Failure analysis, crack propagation among others.

Implicit calculations can also be performed using LS-DYNA solver.

6.2 Elements

For this work, shell, TShell, beams and solid elements are used. To model the entire structure of the roll cage to apply FIA test conditions Beam elements are used. For the detailed model of the mounting, shell elements are used to model the tube and solid elements for the bolts and thick shell elements for the plates. Plates are modelled using thick shell elements as they are subjected to out of plane loadings and it is important to have a good behaviour of this phenomenon on the model.

6.3 Contact

The modelling of the contact is an important factor on this analysis. The model contains several features such as plates and bolts that make contact to each other and is necessary to obtain a good response of the contacts on the simulations. To obtain those forces the cards

CONTACT_AUTOMATIC_SURFACE_TO_SURFACE and CONTACT_FORCE_TRANSDUCER are used along with the DATABASE_RCFOR to extract the readings of force at the specified intervals. [7]

6.4 Bolts and Bolts Preload

The modelling approach used in this work is to model the bolt and nut as a whole using solid elements. The reason for using solid elements is that the pre stress can only be applied to this kind of element. Then an initial stress is applied to the bolt shank which compresses the plates applying an initial compressive loading to the plates. This process is done using dynamic relaxation in the initialization phase of the simulation. The initial stress acts on the bolt shank and when that process reaches equilibrium given the predefined conditions for equilibrium, the structural analysis starts. On the following image the FE Model created is presented. Two plates are tied together using a single bolt connection similarly to [8].

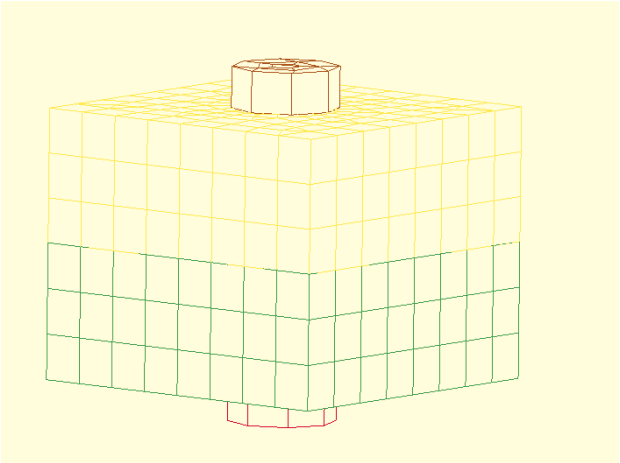

6-1. Bolted joints model

The preload has to be calibrated by iteration of the stress value. In this simple example a preload of 12kN is obtained using a 200Mpa stress on the bolt shank. Then, an increasing force T is applied to separate the plates.

The following graph 6-2 shows the behaviour of the model created in LS-DYNA regarding the applied force T against the bolt and plated load.

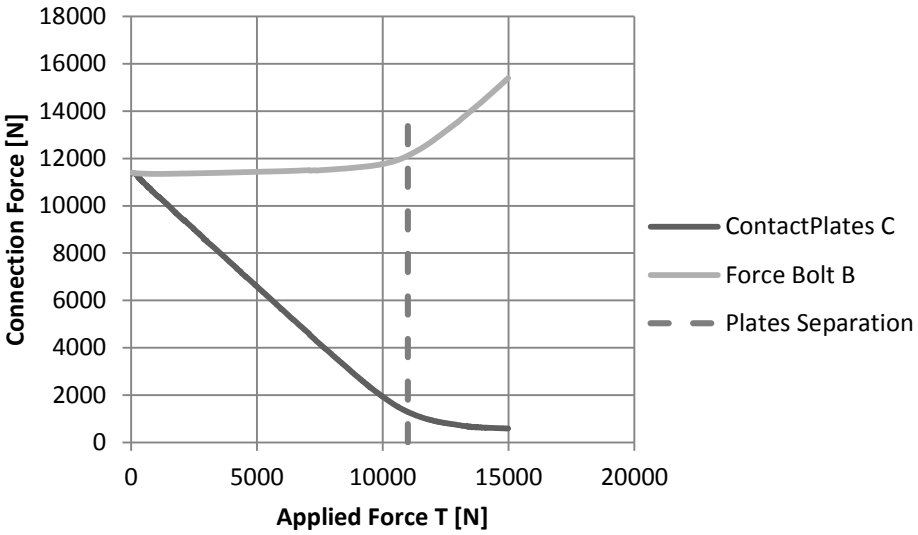

6-2. Bolt and Plates Force vs applied load for prestressed single bolt connection

As observed, the contact force of the plates decrease when the external applied load rises but the load carried by the bolt remains practically constant. When the value of the external force is close to 12kN, which is the applied preload, the force contact of the plates is close to zero. After that point, the external load acts directly on the bolt causing that force B is equal to external force T.

6.5 Plates Modelling

To model the plates of the floor, feet mounting and reinforcement plate the elements solid, thick shell and shell are tested. A simple beam model subjected to bending is created using all the mentioned elements the accuracy of results is checked. It is important that the plates created are able to represent the bending through thickness stress as the most probable mode of failure for the plates is on bending.

The dimensions of the beam are the same for all the models and are the following.

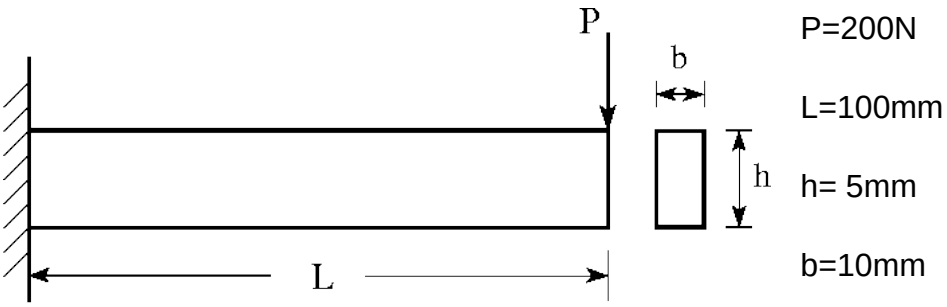

6-3. Cantilever Beam Dimensions

6.5.1 Solid Elements Cantilever Beam

A model using solid elements is created at first and the aspect is the following.

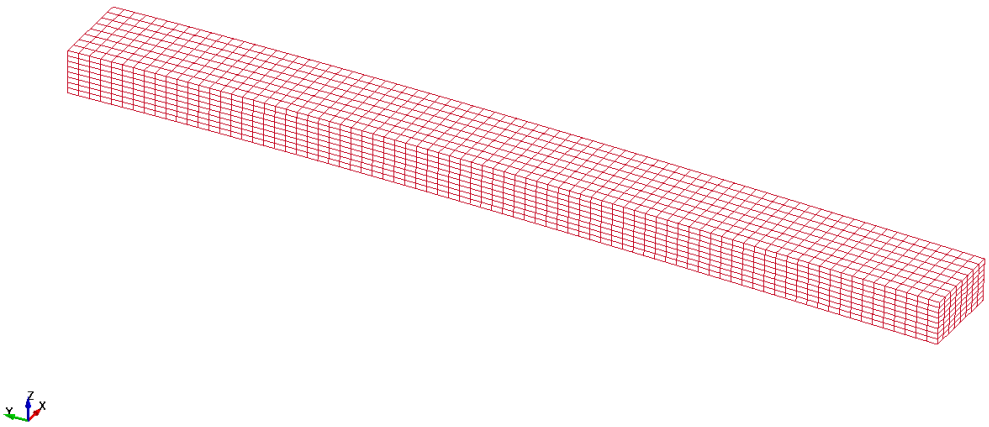

6-4. Solids Cantilever beam

The real length of the beam model is 110 mm but the last 10 mm are fully constrained to represent the encasement. The loading is applied to one node at the centre of the other end and this node is constrained to all the nodes of the end face using CONSTRAINED_NODAL_RIGID_BODY as the following image shows.

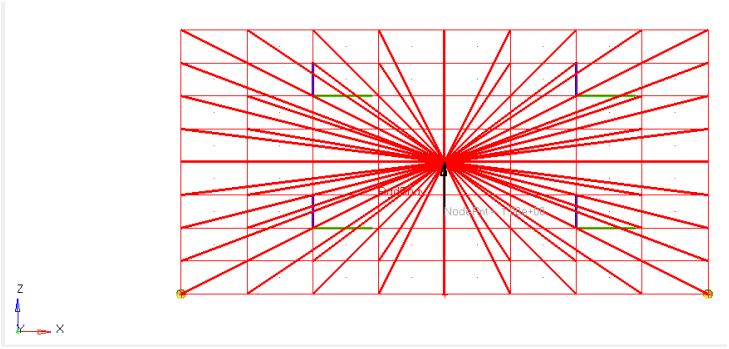

6-5. Nodal Rigid Body

As can be seen, all the nodes contained at the end face are constrained to the central node of the face. With this solution, a force (note black vector on previous figure 6-5) can be applied to the central node and the force is equally distributed on all the nodes.

Through the thickness 8 solid elements are used meaning that for each layer of solids there will be 8 output results as each element has one integration point. The results extracted from this simulation are the local x stresses at the encased end solids layer.

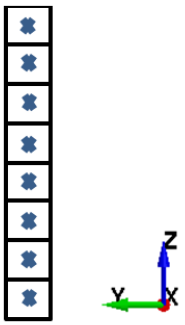

6-6. Through Thickness Solid Elements Integration Points

The y stress results for the previous figure integration points are obtained. Then, the results obtained are compared to beam theory stress values.

IP	Y Coordinate [mm]	Stress Y Direction (Simulation) [MPa]	Stress Y Direction (Analytical) [MPa]	ERROR ABS (%)
8	2,1875	459	420	9,29
7	1,5625	307	300	2,33
6	0,9375	180	180	0,00
5	0,3125	57,7	60	3,83
-	-	-	0	-
4	-0,3125	-62,8	-60	4,67
3	-0,9375	-185	-180	2,78
2	-1,5625	-313	-300	4,33
1	-2,1875	-467	-420	11,19
			AVERAGE ERROR	**4,8**

Table 6-1. Solid Elements / Analytical Results Error

An average error of 4,8% is obtained. The integration points location is assumed to be exactly in the middle of the solid elements and the analytical solution is calculated using the distance of the integration point to the neutral plane.

The computational time for this simulation is 45 minutes approximately.

6.5.2 Thick Shell Elements Cantilever Beam

The Cantilever beam is also modelled using thick shell elements. These elements are 8noded elements where the through thickness integration points can be defined. The advantage of these elements respect the solid elements is that for one element of thick shell elements the results on the integration points can be obtained while in the solid elements there is only one integration point per element.

That means, for example, that to reflect the stresses through thickness on a cantilever beam are needed at least 3 solid elements, one for the tension side, another for the neutral plane and at least another one for the compression side. In the following figure 6-7, 4 integration points through thickness are used on both solids and TShell elements.

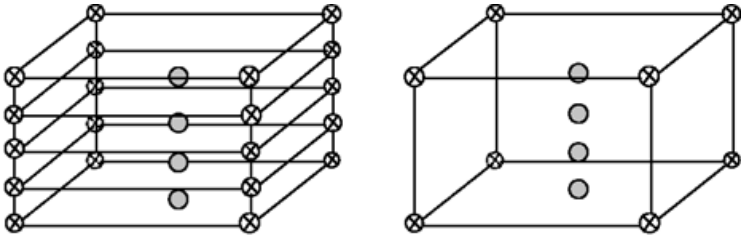

6-7. Solid Element and Thick Shell Element (4IP)

Using thick shell elements the beam can be modelled using only one element through the thickness with three integration points. On both approaches three integration points through thickness are achieved but the computational time for the thick shell solution is significantly lower.

To test this modelling solution, two approaches for the cantilever beam are created. The first approach is using 2 TShell elements with 5 IP each doing a total of 10 IP through the total thickness of the beam. The second approach is using only one element through thickness with 10 IP achieving the same amount of total integration points on both models.

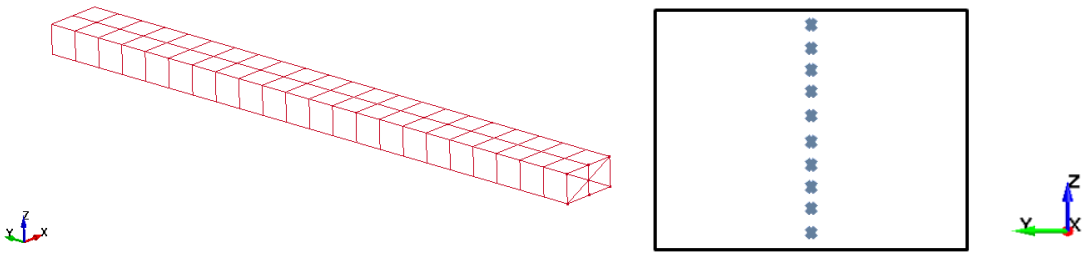

6-8.TShell 1 Element 10IP

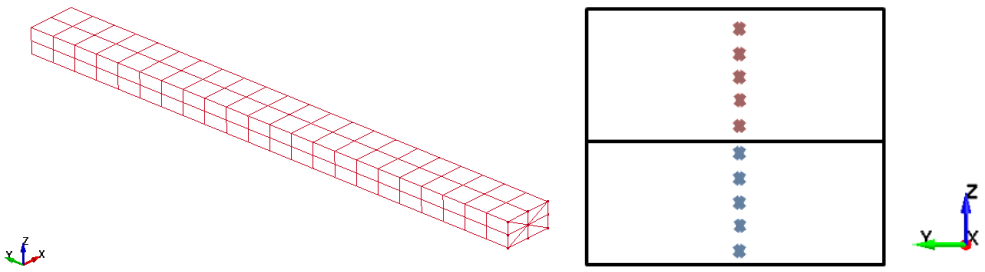

6-9. TShell 2 Elements 5IP

On previous figures 6-8 and 6-9 is shown the cantilever beam model created and the distribution of the elements through thickness integration points.

The y-local stress are obtained on each integration point of the previous figures and compared to the analytical results. The following table shows the results and absolute error for the 1 element 10IP model.

IP	Z Coordinate [mm]	Stress Y (Simulation) [MPa]	Stress Y (Analytical) [MPa]	ERROR ABS (%)
10	2,25	465	410,4	13,30
9	1,75	407	336	21,13
8	1,25	319	240	32,92
7	0,75	203	144	40,97
6	0,25	70,4	48	46,67
-	-	-	-	-
5	-0,25	-69,4	-48	44,58
4	-0,75	-204	-144	41,67
3	-1,25	-319	-240	32,92
2	-1,75	-407	-336	21,13
1	-2,25	-457	-432	5,79
			AVERAGE ERROR	**30.1**

Table 6-2.TShell 1Element 10IP / Analytical Results Error

And in the next table the results for the 2 elements 5IP model are presented.

IP	Z Coordinate [mm]	Stress Y Direction (Simulation) [MPa]	Stress Y Direction (Analytical) [MPa]	ERROR ABS (%)
10	2,25	448	410,4	9,161793
9	1,75	361	319,2	13,09524
8	1,25	236	228	3,508772
7	0,75	111	136,8	18,85965
6	0,25	25,8	45,6	43,42105
-	-	-	0	-
5	-0,25	-19,6	-45,6	57,01754
4	-0,75	-106	-136,8	22,51462

3	-1,25	-237	-228	3,947368
2	-1,75	-366	-319,2	14,66165
1	-2,25	-453	-410,4	10,38012
			AVERAGE ERROR	**19.65**

Table 6-3. TShell 2 Elements 5IP / Analytical Results Error

The computational cost is 2 minutes 30 seconds for the 1 Element model and 5 minutes for the 2 Elements through thickness model.

The results regarding computational time and accuracy of solutions are compared in the following table.

MODEL	ABS ERROR (%)	CPU TIME
1-SOLIDS (8 Elements)	4.8	45 min
2- TSHELL (1 Element)	30.1	2.5 min
3- TSHELL (2 Elements)	19.65	5 min

Table 6-4. Accuracy vs CPU Cost

A model with error higher than 20% will be considered a wrong modelling approach to reflect bending. In this case, model 2 presents a 29% error meaning that the model is rejected. An aspect that must be taken into account is that the error on TShell models is very high on the points closer to the neutral plane of the cantilever beam. Those big error produce an average error quite big also. On the points of interest of the beam, the maximum stress points the errors are around 10 % meaning that for the purpose of the models (failure) Tshell elements would do the job.

7 TUBE MODEL VALIDATION

To create the FE model of the tubes used in the roll cage, test results from previous thesis are used, Godillon [9]. The experiment consists of a quasi-static test performed to a clamped tube on one end while the other end is displacement controlled. At the clamped end of the tube a plastic hinge will appear as the moment at that point is the highest. The test data available is from tubes of the following sections:

Ø 38.1 mm, t=1.828 mm

Ø 38.1 mm, t=1.018 mm

Ø 38.1 mm, t=1.219 mm

And the used material specifications for the cold drawn steel T45 are the following:

0,2% proof stress 600-660 MPa

Ultimate yield stress: 700-900 MPa

Elongation at failure: 26%

Young Modulus: 180000-210000 MPa

7.1 Test Data

Below are reproduced the curves obtained from test data.

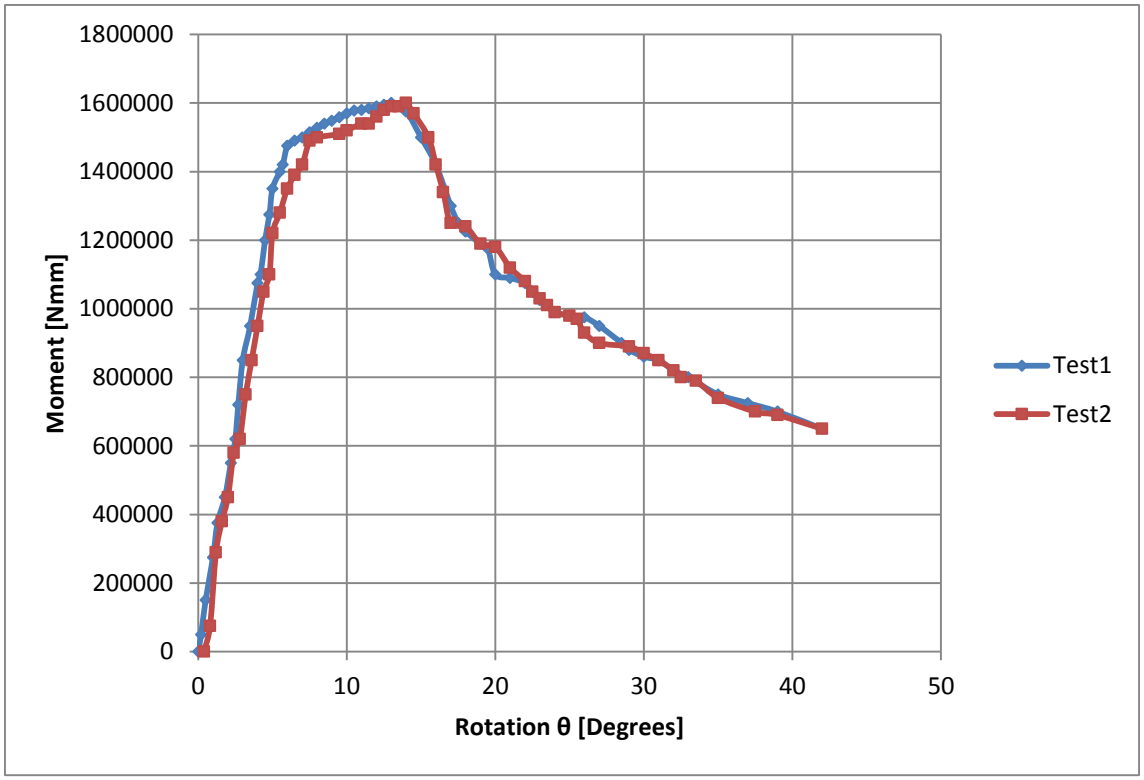

7-1. Test Results Ø38.1mm t=1.828mm [9]

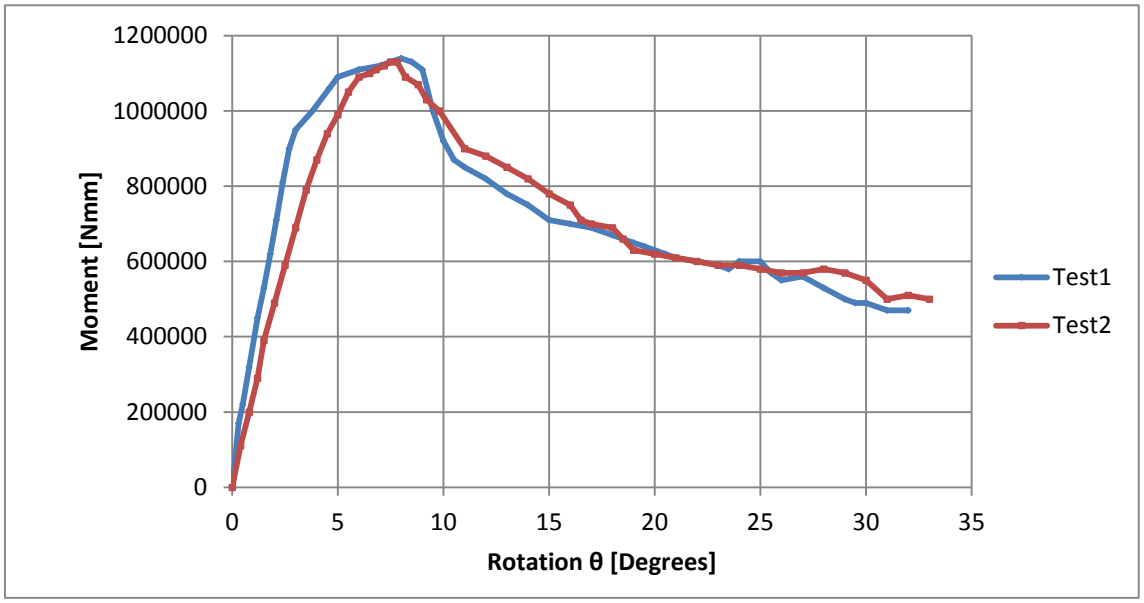

7-2. Test Results Ø38.1mm t=1.216mm [9]

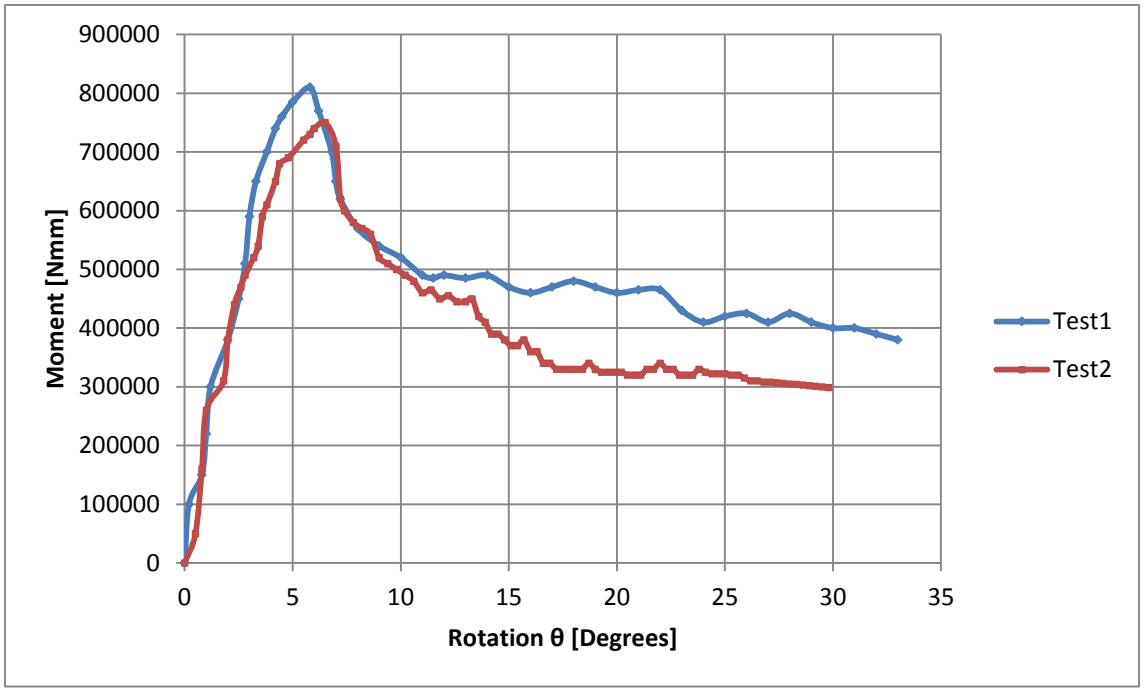

7-3. Test Results Ø38.1mm t=1.016mm [9]

7.2 FE Model

Using the test curves to validate the model, a finite element model of the tubes is created. The following image corresponds to the tube specimen using mesh size 3 on the plastic hinge section at the bottom of the tube. The tube is fully constrained at the base nodes. A velocity is applied on top of the tube using a NODAl_RIGID_BODY on the nodes on top.

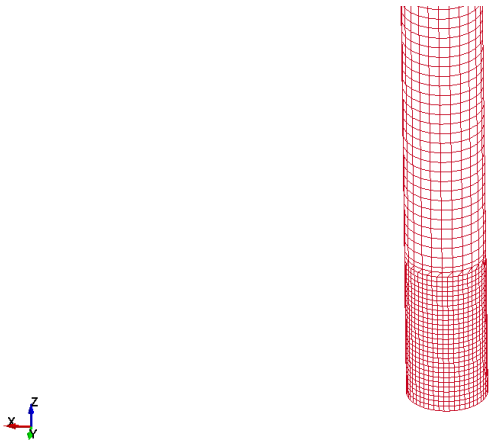

7-4. Tube FE Model

As the material data available is only the specification of the material and not the actual material properties of the tubes, a sensitivity analysis of the material will be performed. Initially the data used for the material is the specified on the previous work [9].

Regarding other aspects of the model a mesh size, element formulation and number of integration points sensitivity study is also done to obtain an accurate modelling of the tube.

7.2.1 Mesh sensitivity

Initially a 5 size mesh is used all along the tube. Then the tube is refined at its base, where the plastic hinge occurs and the accuracy is more important. To perform this analysis the tube used us the 38.1mm diameter and 1.828mm thickness. The results for the moment rotation response of the tube are the following, where mesh 5, mesh 3, and mesh 2, refers to mesh size 5mm, 3mm and 2mm respectively.

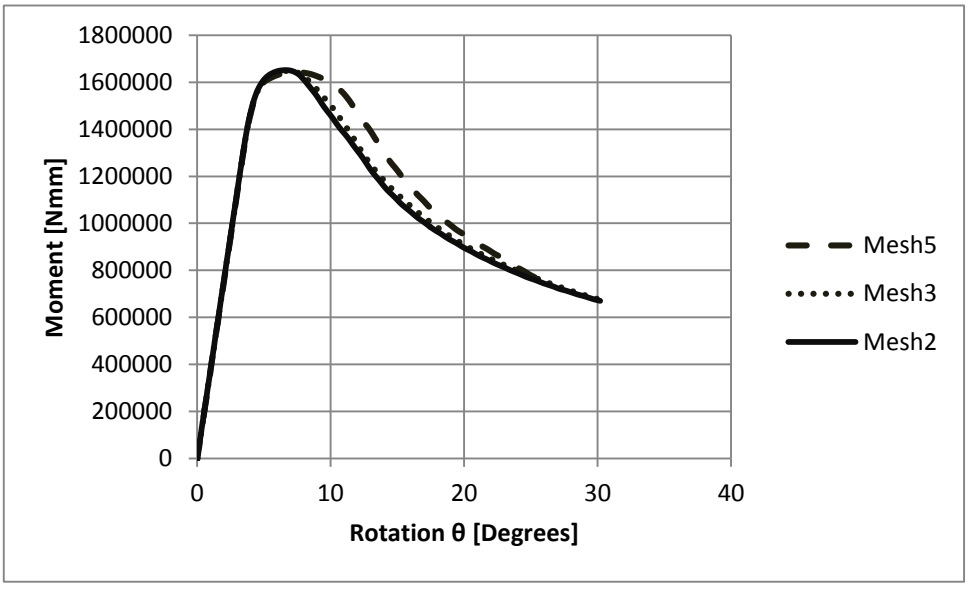

7-5. Tube Mesh Sensitivity Analysis

As observed on the previous results, mesh sizes 2 and 3 present similar results regarding the moment rotation response of the tube. While the CPU time required for the mesh 2 size is around 20 minutes, the calculation time for the mesh 3 sizes is 5 minutes. At the sight of the results it is preferable to use the bigger size

mesh 3 for the modelling of the tube as later this tube model will be introduced into a bigger model. Using this mesh size the results are similar to a more refined mesh and the computational time is 4 times lower.

7.2.2 Material Sensitivity

Young Modulus

The elastic modulus of the steel can vary from 180 up to 210 GPa. The range of uncertainty of the tube material is then quite wide. For this reason 3 different levels of young modulus are simulated: 180, 200 and 210 GPa. And the elastic part of Moment-Rotation curves obtained are compared with the Moment-Rotation curves of the tests.

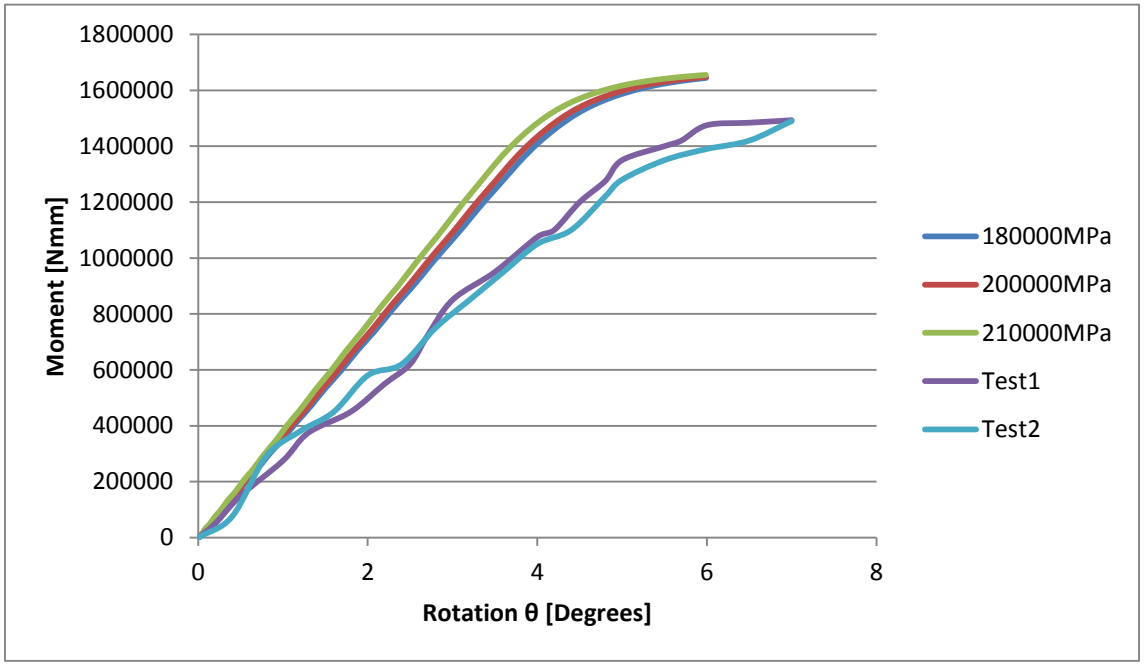

7-6. Tube Elastic Modulus Sensitivity Analysis

Analysing the previous results, the 180 GPa curve is the closest to the testing curve. Although there is a big error between the testing curves and simulation it can be due to the clamping mechanism of the rig commented later. The young modulus used for further simulations is the lowest, 180 GPa.

Yield Stress

As in the case of the Young Modulus, the yield stress can also vary in a certain range of values. In this case the values can vary from 600 to 660 MPa. Using the previously decided young modulus, the curves for 600, 620, 640 and 660 MPa as yield stress are obtained.

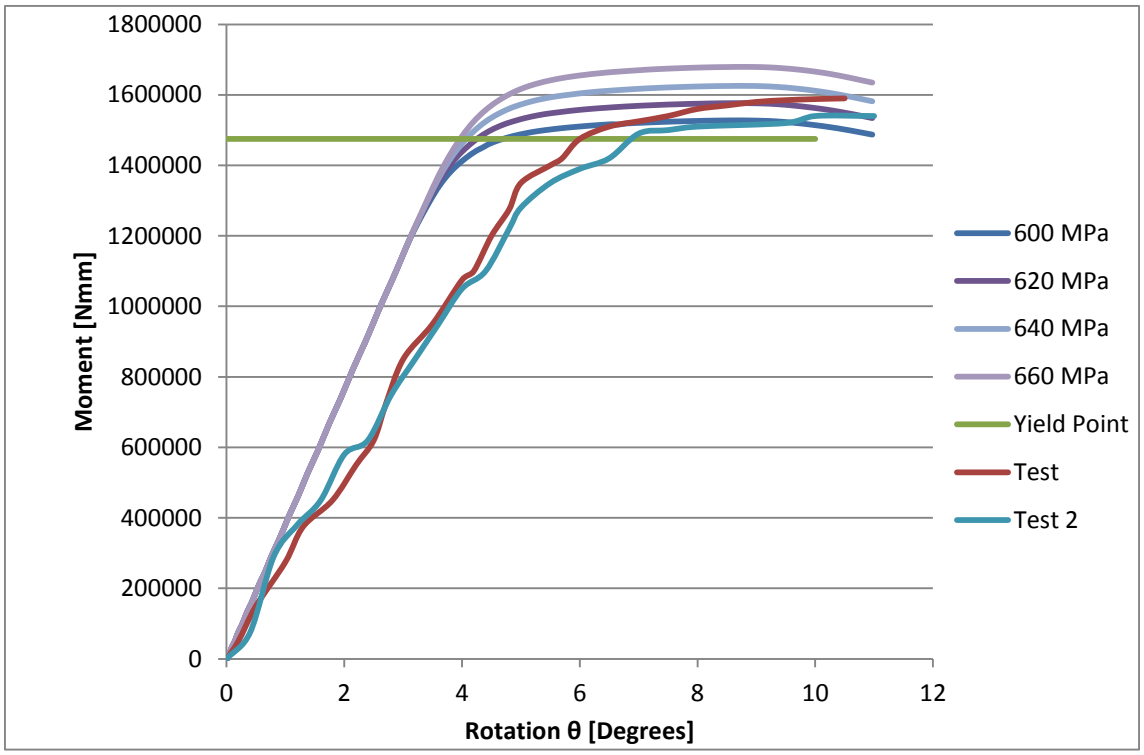

7-7. Tube Yield Stress Sensitivity Analysis

Observing the results and comparing the simulation with the test, the yield point of the curve 620 MPa appears to be the closest to the test results (see Yield point line). For this reason it is decided to use 620 MPa as the yield stress of the material T45 for further simulations.

Ultimate Stress

Finally, and using the yield stress obtained previously, an ultimate stress sensitivity analysis is performed. Three levels are chosen: 700, 800 and 900 MPa. The results compared with the test results are the following.

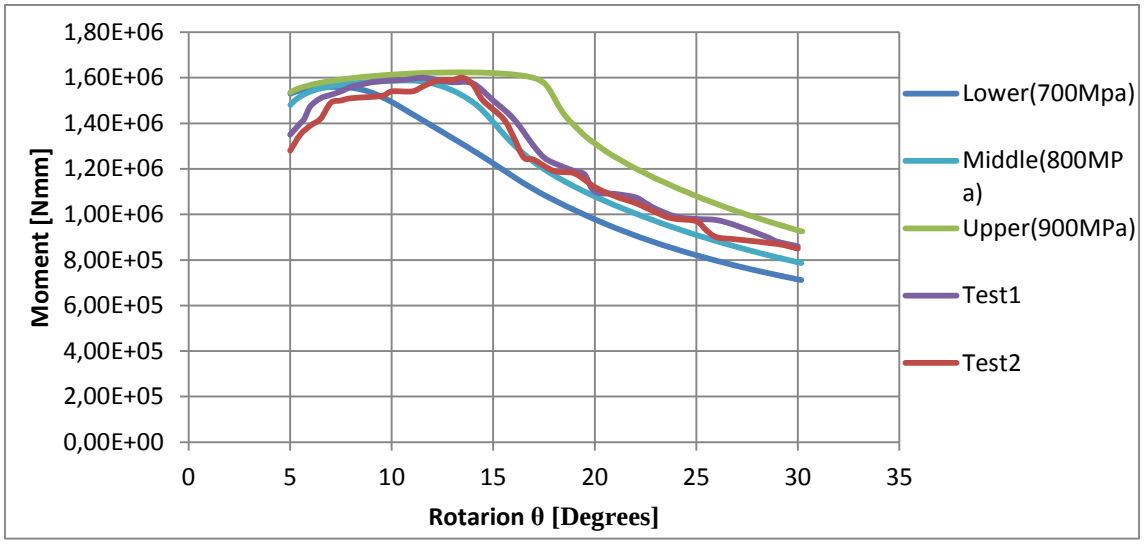

7-8 Tube Ultimate Stress Sensitivity Analysis

This parameter influences in the level of increment of the resisting moment after plastic collapse has occurred. For example, for the lower level of the parameter the curve immediately decreases after reaching plastic deformation. For the middle value the curve top part is closer to the test result and the parameter of the simulation is used for the material properties.

This material sensitivity analysis is performed to have an idea of what is the range of error that can exist if the exact material properties are not know and only the material specification is given. For a same material specification a wide range of values can be used and at the sight of the results presented above they are very different from one to another.

7.2.3 Correlation of Results

The Moment-Rotation curves obtained from both test and simulation are plotted in the same graph to observe the accuracy of results. Also, using the work done by S.Poonaya [10] a theoretical bending collapse curve is obtained and compared with the test and simulation results.

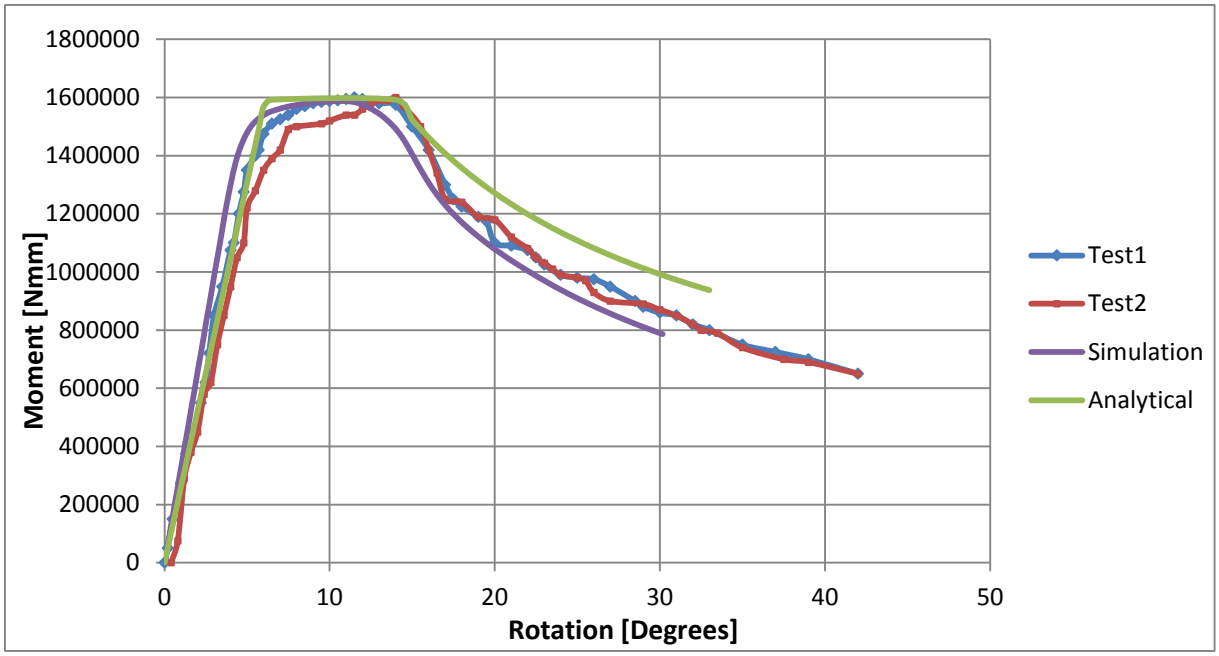

7-9. Moment-Rotation Curves Ø 38.1 mm, t=1.828 mm

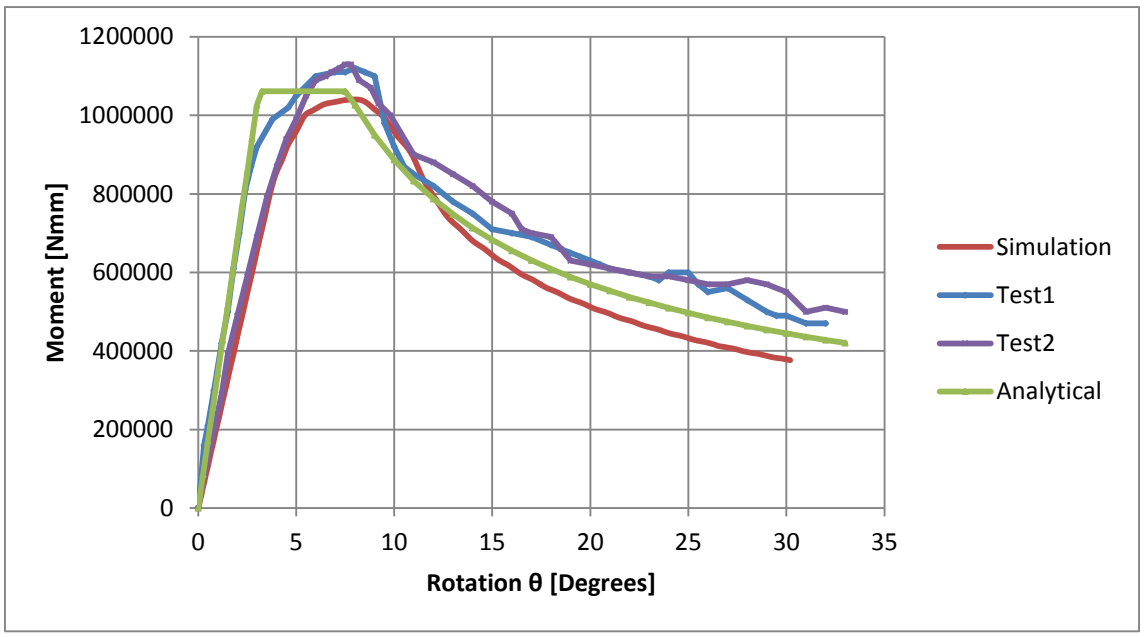

7-10. Moment-Rotation Curves Ø 38.1 mm, t=1.018 mm

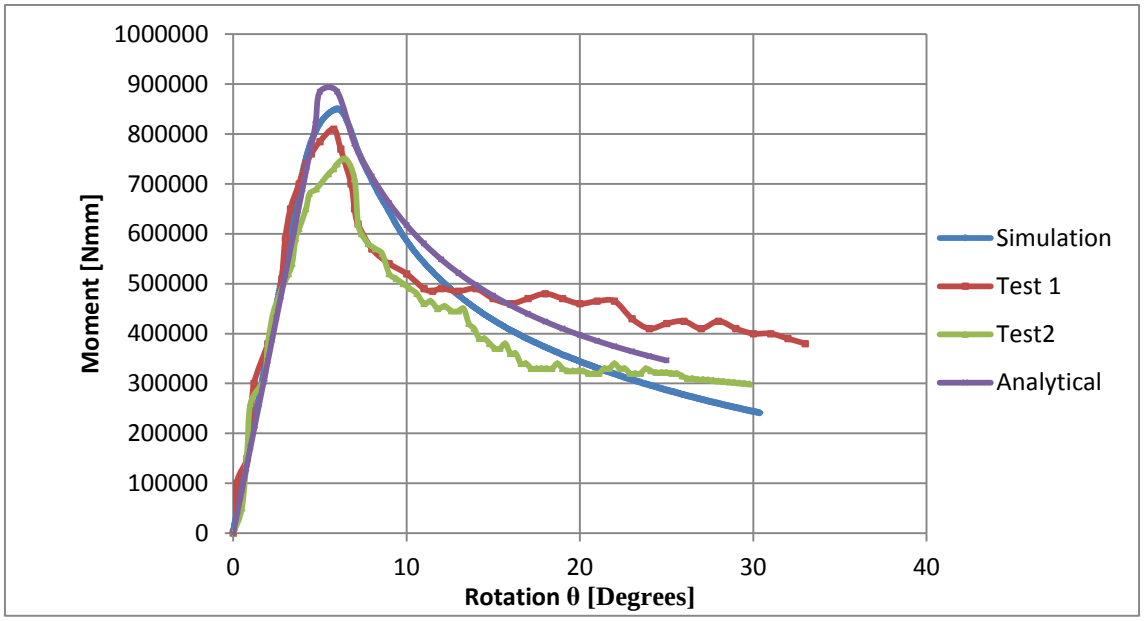

7-11.Moment-Rotation Curves Ø 38.1 mm, t=1.219 mm

At the sight of the previous graphs it is clear that a good correlation between hand calculation, simulation and test is achieved. For the thinner tube specimen there is a big discrepancy on the maximum resisting moment between all cases.

7.3 Roll Cage Mounting Model Tube

Tubes used in the roll cage are generally of dimensions Ø 44.45 mm, t=2.64 mm and material cds 355N as stated on section 4. Previous work using previous test results is done to produce a good model of this tube and compare with the analytical solution. Previously is demonstrated that if the analytical solution is close to the simulation curve it will be also close to a test curve, see section 7.2.3. For this new dimension of the tube a new sensitivity analysis regarding the mesh, number of integration points and loading rate is performed. The results are presented in the following graphs.

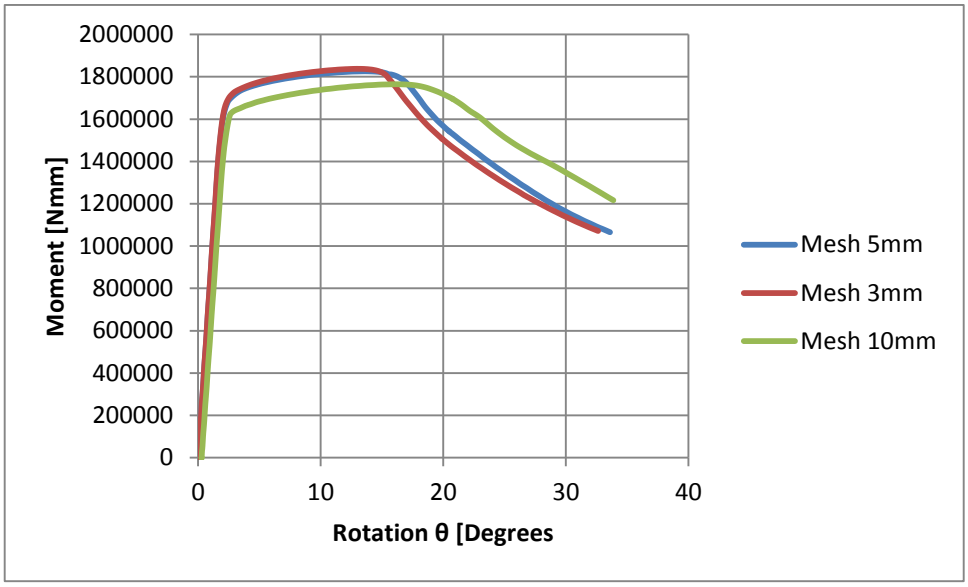

7-12. Mesh Size Sensitivity Analysis

Observing the results of the mesh sensitivity analysis it is clear that a size 10 elements is not suitable to model this tube. For the smaller sizes checked the curves are quite similar and converge. The decision made is to use 5mm elements to not increase the simulation time, as this tube model will be implemented into a bigger model of a mounting.

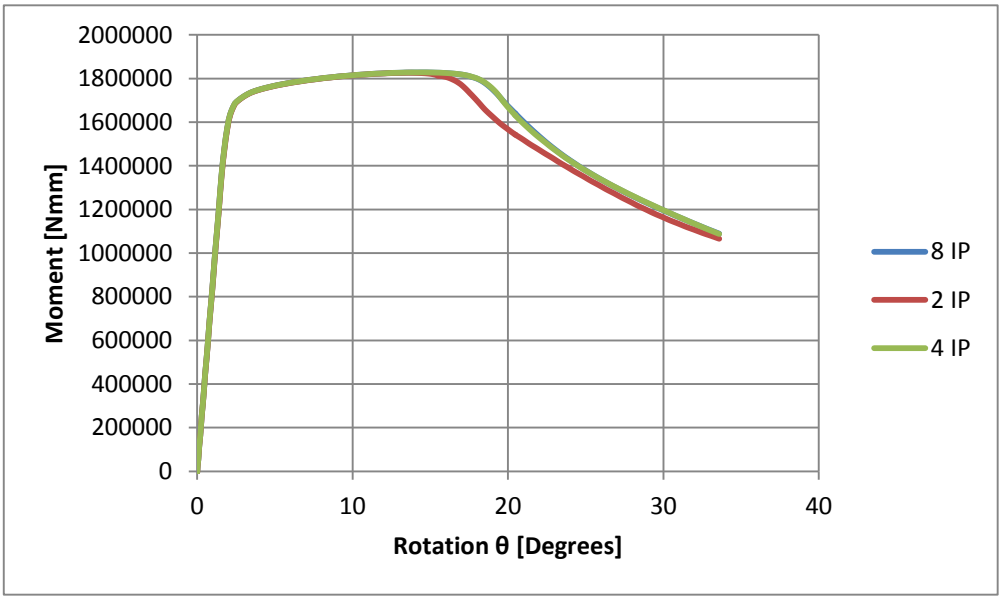

7-13. Integration Points Sensitivity Analysis

The moment rotation curves for different shell integration points are plotted. When using a value higher than 2 IP such as 4 or 8 the curve converges. At the sight of the results, 4 IP will be used on the tube modelling.

Finally a load rate analysis is performed to check if the velocity of the bending influences the resisting moment curve.

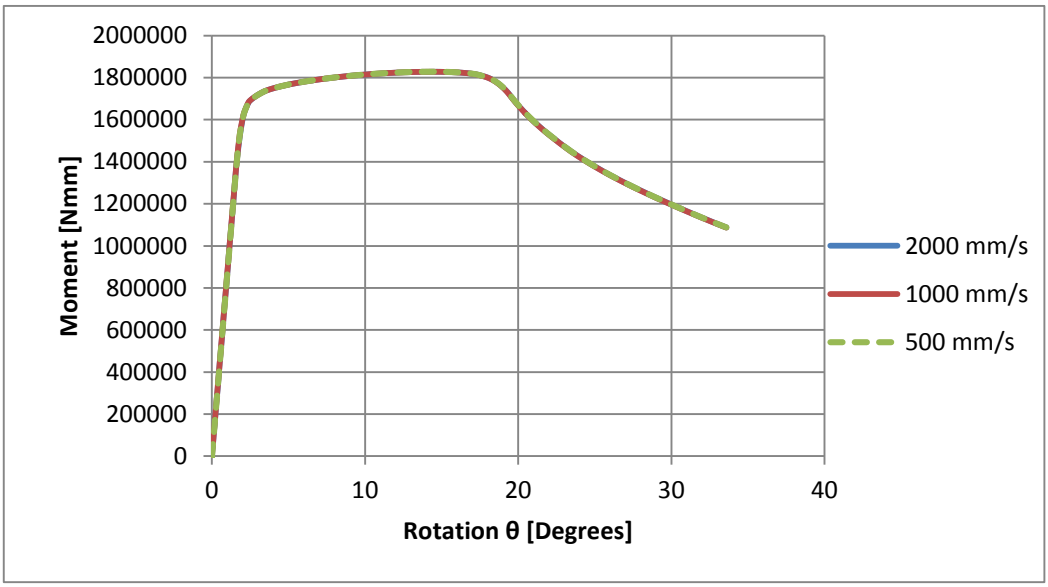

7-14. Load Rate Sensitivity Analysis

The curves show that the loading rate does not affect the simulation results. From now on, for the tube it will be used the 2000mm/s velocity as the simulation time is lower.

After the sensitivity analysis performed on the tube, the curve obtained is compared with the analytical solution from S.Poonaya et al. [10] used previously. Both curves are plotted on the same graph and the accuracy of the results is discussed.

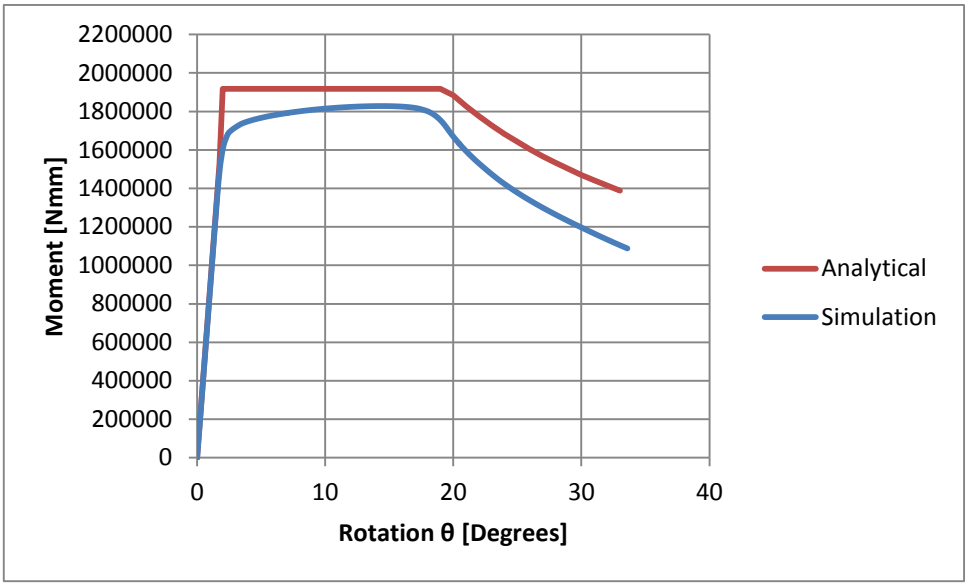

7-15.Simulation and Analytical Moment-Rotation Curves Ø44.45 mm, t=2.64 mm

The discrepancy between the analytical and the simulation curves is around 5% of error at the maximum points. In conclusion, a good modelling for the tubes of the roll cage is achieved and this model will be used as part of the final models.

8 SIMULATION OF ROLL CAGE FIA TEST

In order to have an idea of the approximate forces that the mountings in a roll cage experience in a FIA test, a simulation of those tests is performed. For this part of the project beam elements are used and therefore this type of element must be validated to make sure the roll cage is behaving correctly under the test loadings.

8.1 Beam Tube Validation

A cantilever beam of the same circular section as the roll cage tubes is created and a bending moment is applied. The FE model presents the following aspect.

Material used is CDS E355N using *MAT_ 24 on LS-Dyna.

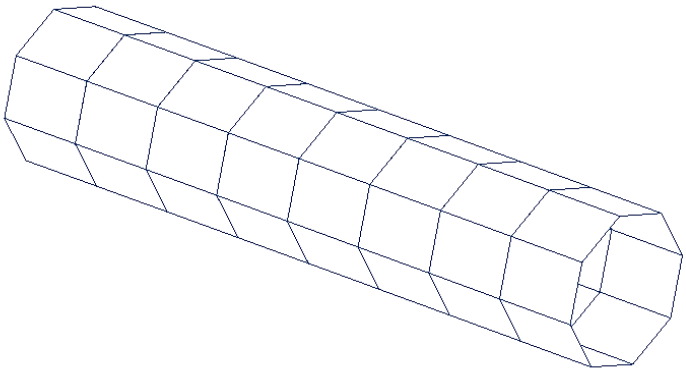

8-1. Cantilever Beam Simple Model

The model consists of a 200mm long beam formed by 25mm long beam elements doing a total of 8 beam elements. Section of the beam parameters used are 44.45mm outer diameter 1.32mm thick. On one end the node is fully constrained on all translational and rotational degrees of freedom and on the other end a z-direction 2000N force is applied.

To check if the model is behaving correctly, the maximum stress at the clamped beam element at the midpoint and the maximum vertical displacement are compared against analytical solutions.

Maximum stress of the beam is calculated using beam theory equation used previously on the thick shell elements validation as follows.

$$\sigma_{MAX} = \frac{M * y}{I} = \frac{2000N * 187.5mm * 22.225mm}{4.1627x10^4 mm^4} = 200.21MPa$$

Where:

- M is the moment at the point of interest.
- y is the cross section coordinate location of the point of interest.
- I is the second moment of area.

A maximum stress value of 193N is obtained on the simulation which means that an absolute error of 3.5% is made compared with analytical value.

The model is also validated reading the maximum displacement on the beam and comparing the result with theoretical value. To calculate the value the displacement expression of a cantilever beam as the following is used.

$$\delta = \frac{PL^3}{3EI} = \frac{2000N \cdot 200^3 mm}{3 \cdot 210000MPa \cdot 4.1627x10^4 mm^4} = 0.61mm$$

The analytical solution provides a value of 0.61mm. Simulation displacement result is 0.638mm. Error committed by simulation is 4.5% in absolute terms.

At the sight of the previous validations, the way the beams are modelled is correct and the behaviour of those elements is the expected by analytical solutions.

8.2 Roll Cage Model

An .igs file is received from the company containing the wireframe of the roll cage. This model is then modified to create the FE model. For example, the bends of the tubes are simplified in order to have fewer nodes on those zones and in consequence less elements when meshing. The following image shows how the bends are modelled.

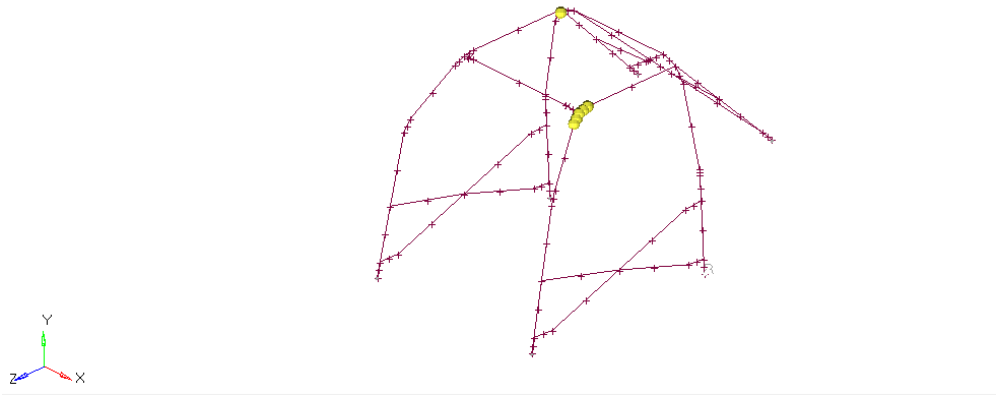

8-2. Wireframe Model

Once the wireframe is modified, beam elements are created using the card property SECTION_BEAM. Hughes-Liu with cross section integration formulation is used. Cross section type is set to tubular which allows to input the inner and outer diameter at each end nodes of the beams. In this case, to model a tube of diameter 44.45mm and thickness 2.64mm, the parameters 44.45mm and

39.17mm are introduced as outer and inner diameter respectively. Also, the maximum length of a beam element is set to 350mm to ensure that the roll cage is not behaving too rigidly as a result of a coarse mesh.

The material used is the indicated by the company, cold drawn steel 355N.

As demonstrated previously, this modelling of the beams is validated and have a correct behaviour.

The rotation and translation degrees of freedom of the points attached to the car are fully constrained.

8.3 Front Windscreen Test

A simulation reproducing the test applied at the top of the windscreen is performed. A moving rigid wall acts on the structure as indicated on safety devices technical information section [5]. The existing information regarding this test is very poor and the point of exact application of the force is not clear.

The images below show the initial end final aspect of the roll cage test and the points where plastic deformation occurs.

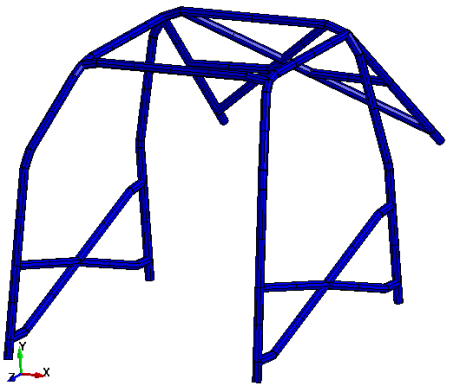

8-3. Roll Cage FE Model

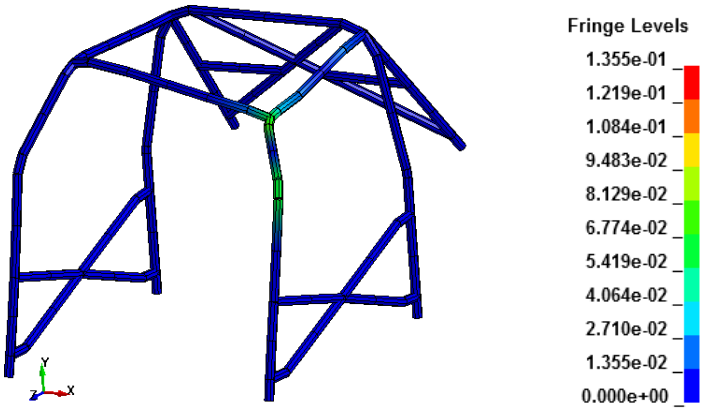

8-4. Roll Cage Front Windscreen Test. Plastic Strain

The deformation occurs mainly in the A pillar and the roof beams closer to the rigid wall actuator. The reaction forces at the rigid wall are extracted and the results are the following.

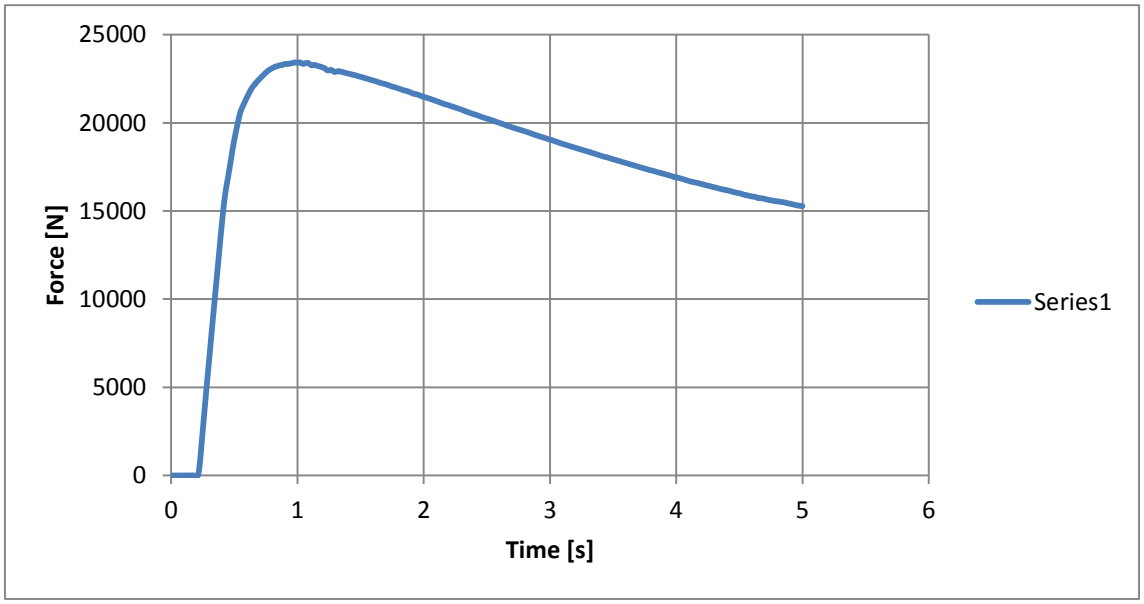

8-5. Rigid Wall Force Windscreen Test

The maximum resisting force of the roll cage is around 24kN. For this test the roll cage should be able to resist a force of 35kN but as there is not clear information about the correct application of the forces this big error can be due to the way the simulation is being performed.

8.4 Main Hoop Test

A similar test is simulated on the main roll bar of the cage. This bar is situated on the B pillars and in reality is formed by a single member. The force that must resist the roll cage on this test is around 75kN.

The images at the initial and final instant of the test are presented below

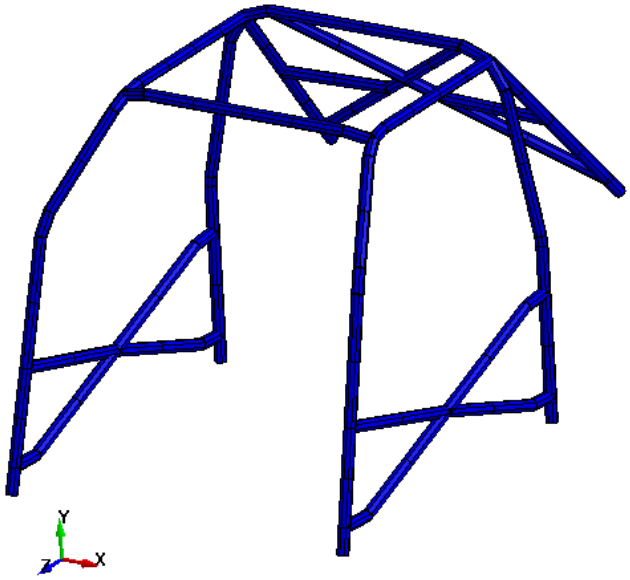

8-6.Roll Cage FE Model

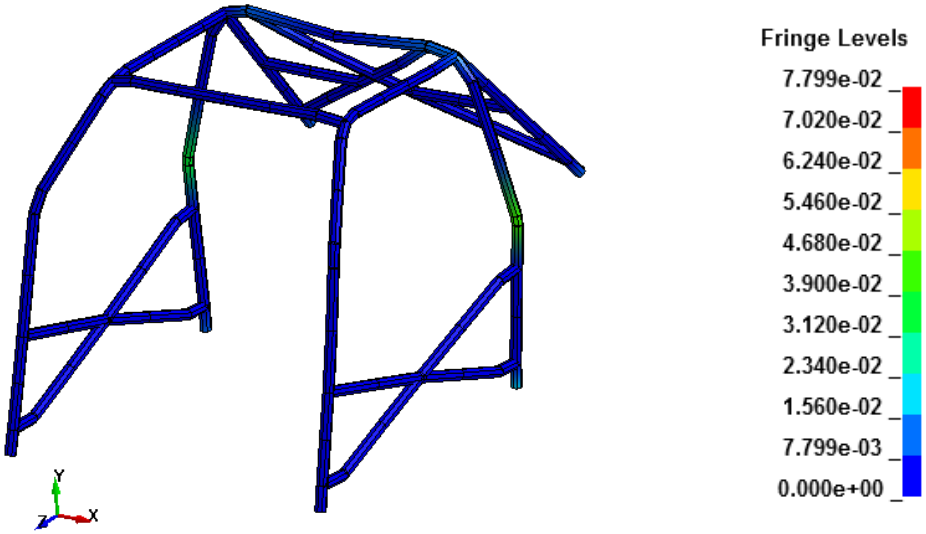

8-7. Roll Cage Main Hoop Test. Plastic Strain

The plastic deformation is produced mainly on the curvature of the B pillar. The following graph shows the resisting force that the roll cage produces to the rigid wall on top of the main roll bar.

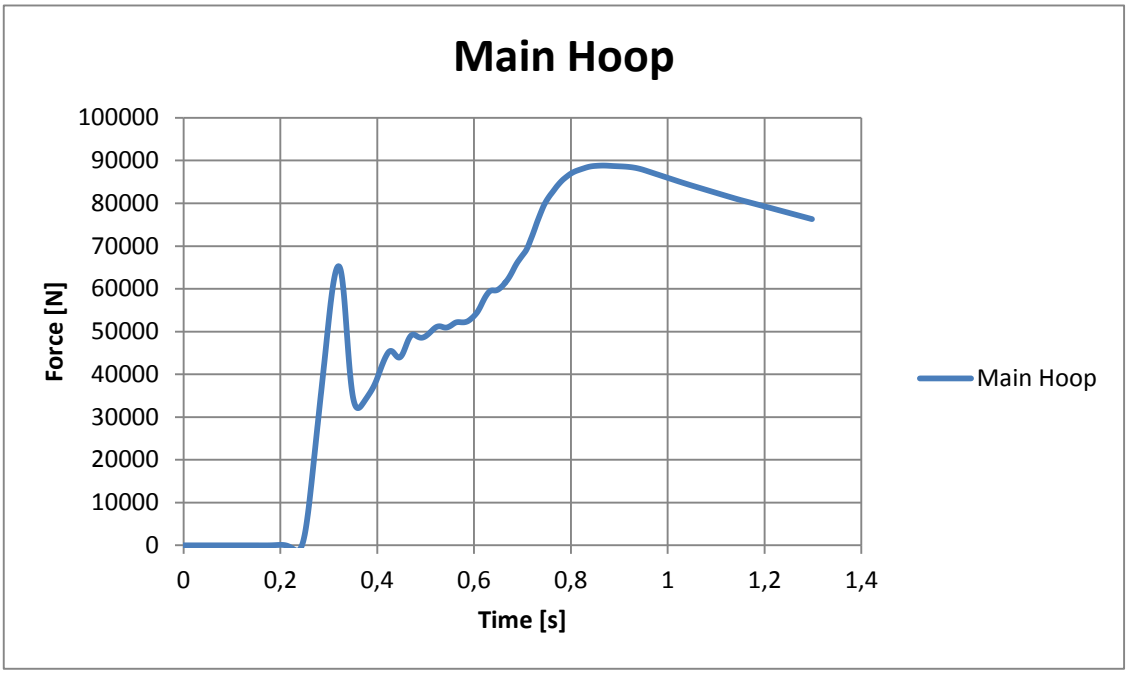

8-8. Rigid Wall Force Main Hoop Test

On this simulation, the maximum force that the roll cage resists is around 90000N. The exact location of the actuator is not precisely known but in this case the roll cage passes FIA test.

8.5 Foot Reaction Forces

The previous tests are performed only to have an idea of the structural loads value that the mountings to the car frame will receive. The highest loaded mounting (A pillar, B pillar or rear pillar) is chosen and the direction of the highest moment is also extracted.

On the following graphs are shown the two principal directions moments applied to the A pillar, B pillar and C pillar of the roll cage on the main hoop test.

S and T directions showed in following graphs correspond to X and Z axes on figure 8-2 respectively.

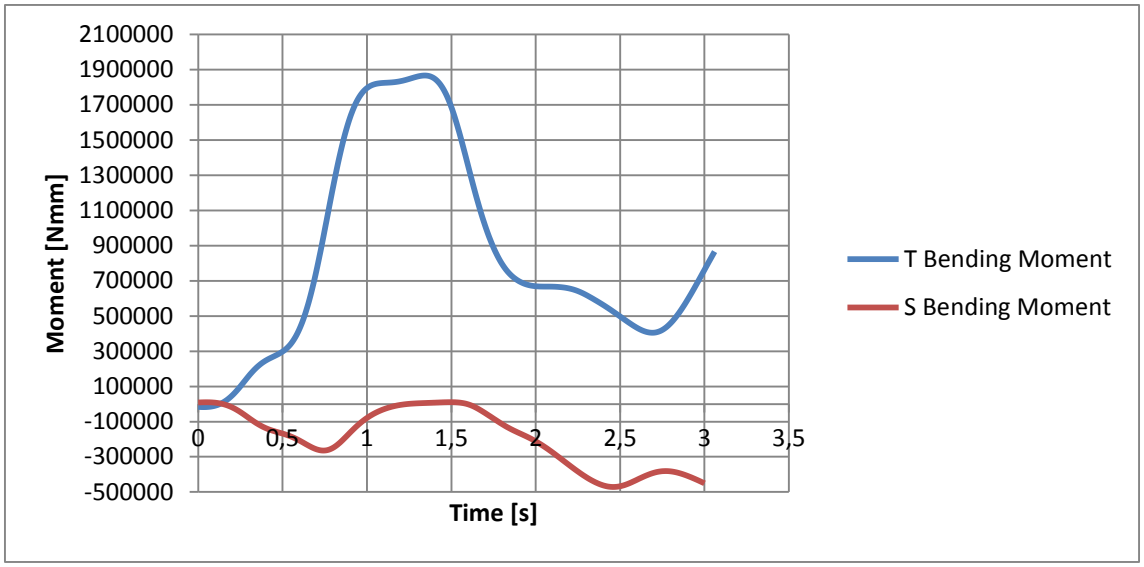

8-9. A Pillar Mounting Bending Moments

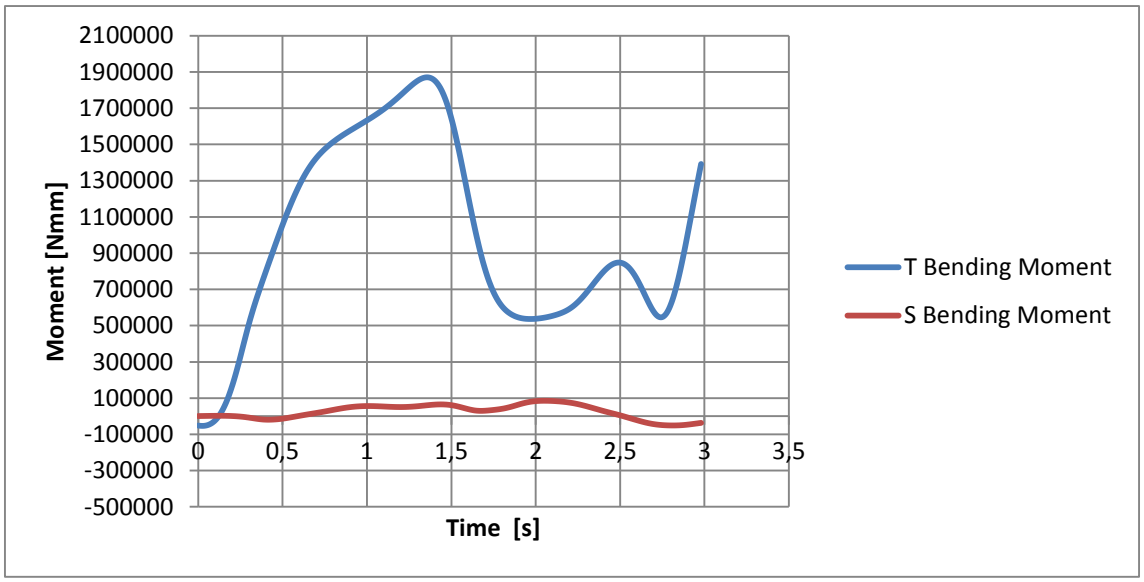

8-10. B Pillar Mounting Bending Moments

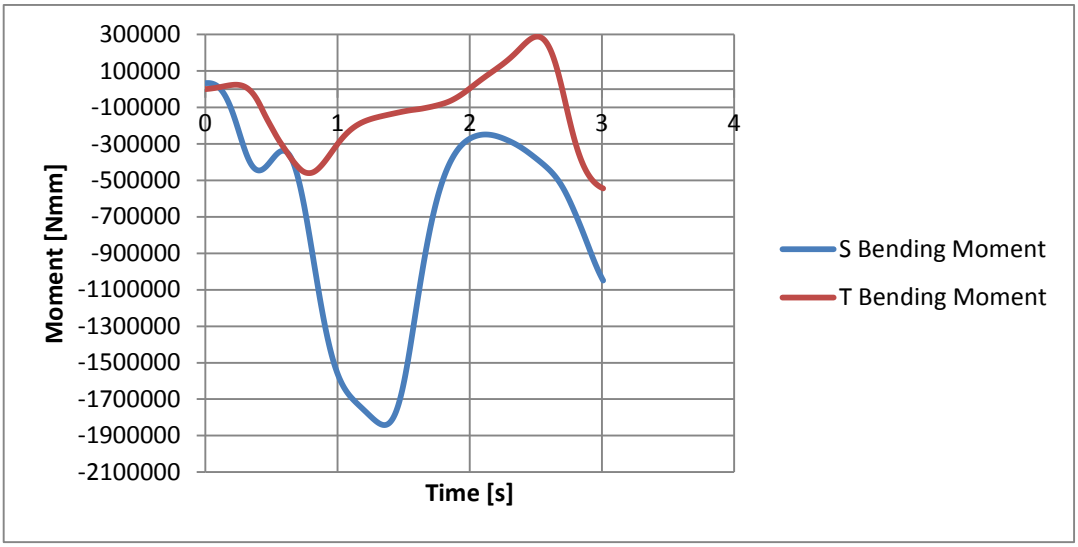

8-11. Rear Pillar Mounting Bending Moments

On all the graphs the maximum moments are close to each other. This result seems to be logical as the roll cage is collapsing on certain points and those tubes are on their maximum resisting moment which is close to that value. In resume, the mounting must be able to resist a moment equal to the maximum collapse moment of the tube as the tube collapse is preferred before a floor and mounting collapse.

9 SIMULATION OF MOUNTING CONFIGURATIONS

9.1 Mountings Modelling

As a reminder of section 4, where all tube models considered are presented, the following table resumes main features of the configurations. Further details on 14Appendix A

Configuration	Features
1 Simply Bolted	Foot plate bolted to floor plate without reinforcement
2 Simply Welded	Foot plate welded to floor plate without reinforcement
3 Bolted	Foot plate welded to floor plate with reinforcement plate underneath
4 Welded	Reinforcement plate welded on top of floor plate, foot plate bolted to floor-reinforcement plates.

Table 9-1. Mounting Configurations Resume

On section 4 is also detailed how on all the configurations the tube is welded to the foot at the centre which is modelled as simply merging the nodes of the tube and foot. This idealised modelling of the weld is done because a weld failure is not expected.

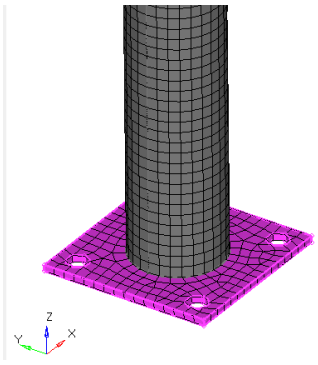

9-1. Tube and Foot Plate FE Model

All models are clamped on the edges of the floor by constraining all degrees of freedom on the nodes of the end edges as the following image shows.

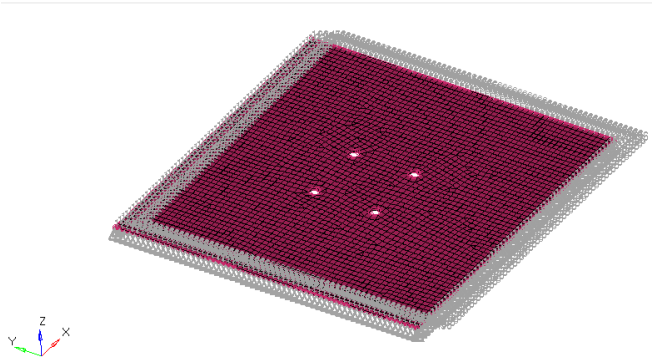

9-2. Floor Plate Edges Constrained

Then contact surface are created for every single surface that is subject of contact and the card CONTACT_AUTOMATIC_SURFACE_TO_SURFACE. After the simulations the contact forces are checked to make sure they are working properly. The checking consist on making sure master and slave surface forces are non-zero, equal and opposite and that the order of magnitude of the forces are similar on all contacts.

Finally, for the models where the reinforcement plate is welded to the floor the card TIED_NODES_TO_SURFACE is used. Edge nodes of the reinforcement directly in contact to the floor are introduced into a set of nodes and used into the tied card to attach them to the floor surface.

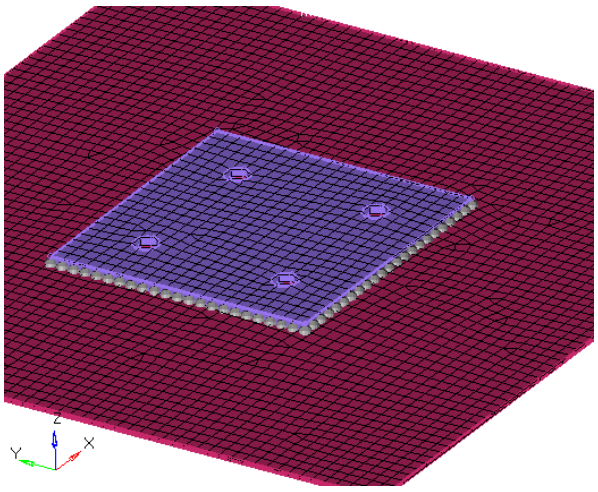

9-3. Tied Nodes Detail. Reinforcement Floor Weld Modelling

Simulations are displacement controlled. On top of the tube a velocity is applied as explained on section 7 for tubes simulations.

9.2 Assessment Criteria

To assess the strength of the designs and compare to each other, a criteria must be defined. In this case three main parameters are observed:

- Maximum resisting moment at the base cross section of the tube.
- Rotation angle at which this maximum moment occurs. Rotation angle is measured using rotation of the top cross section of the tube respect the bottom cross section of the tube at initial position.
- Deformed shape of the mounting when collapsing.

9.3 Foot Bolted Without Reinforcement (C1)

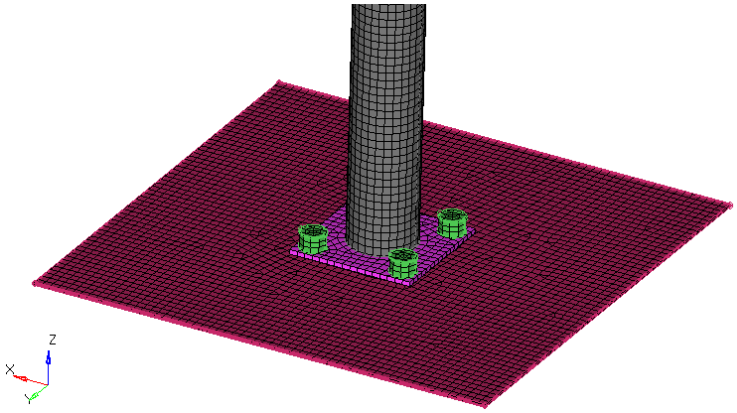

9-4. Bolted Without Reinforcement FE Model

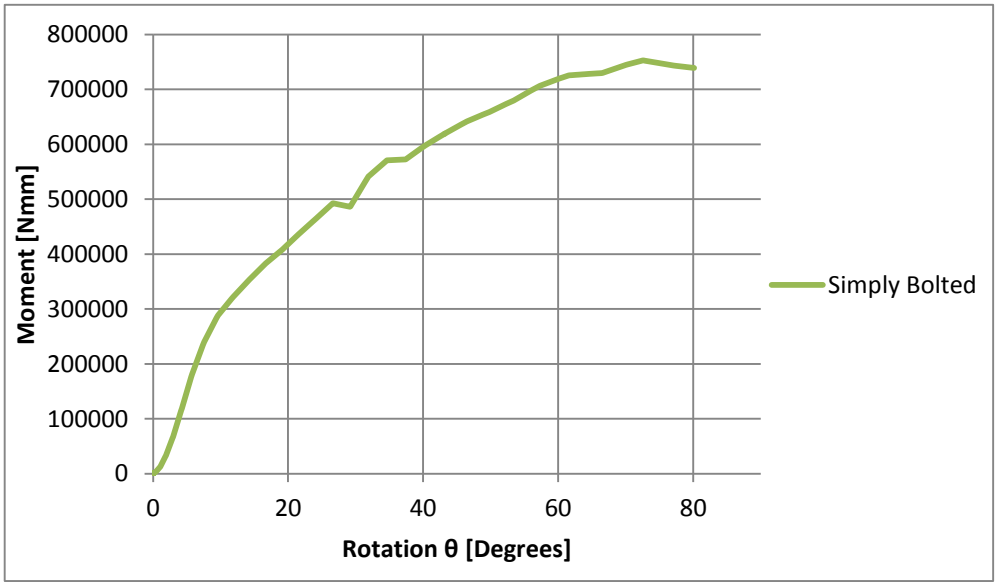

9-5. Moment-Rotation Curve. Configuration 1

On this simulation the maximum moment that the attachment resists is around 750000 Nmm at an angle of 80 degrees. It is clear that this configuration is too far from the desired performance of the mounting. Observing closely at the collapse mode of the mounting on the first stage only the floor starts collapsing (figure 9-6) which is the initial part of the curve. Then, from 10 degrees of rotation on, the foot starts collapsing (figure 9-7) and the resisting moment rises until the maximum observable in the graph. Bolts are pulling up locally the floor. In this case the tube never collapses meaning that the configuration is too weak.

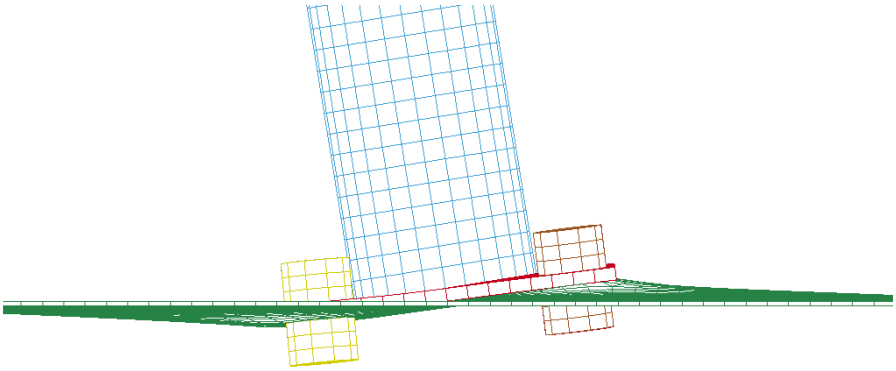

9-6. Floor Collapse. Configuration 1

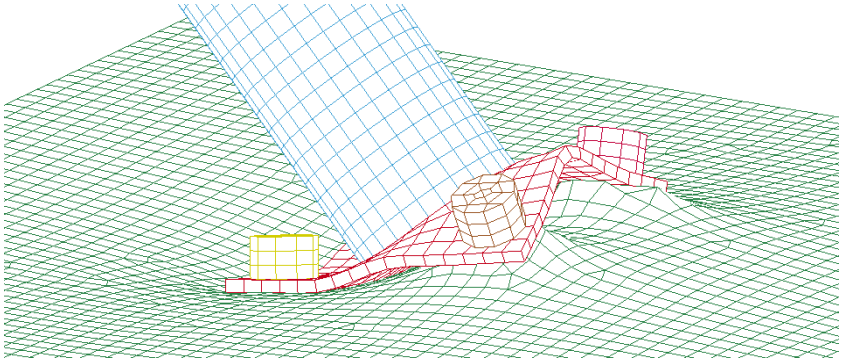

9-7. Foot Collapse. Configuration 1

9.4 Foot Welded Without Reinforcement (C2)

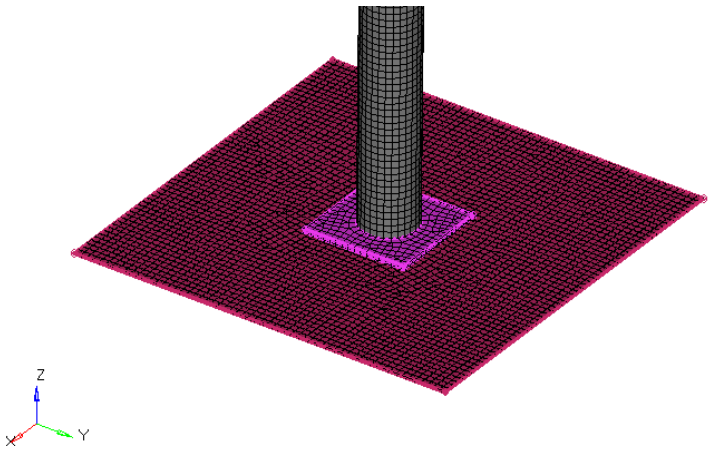

9-8. Welded Without Reinforcement FE Model

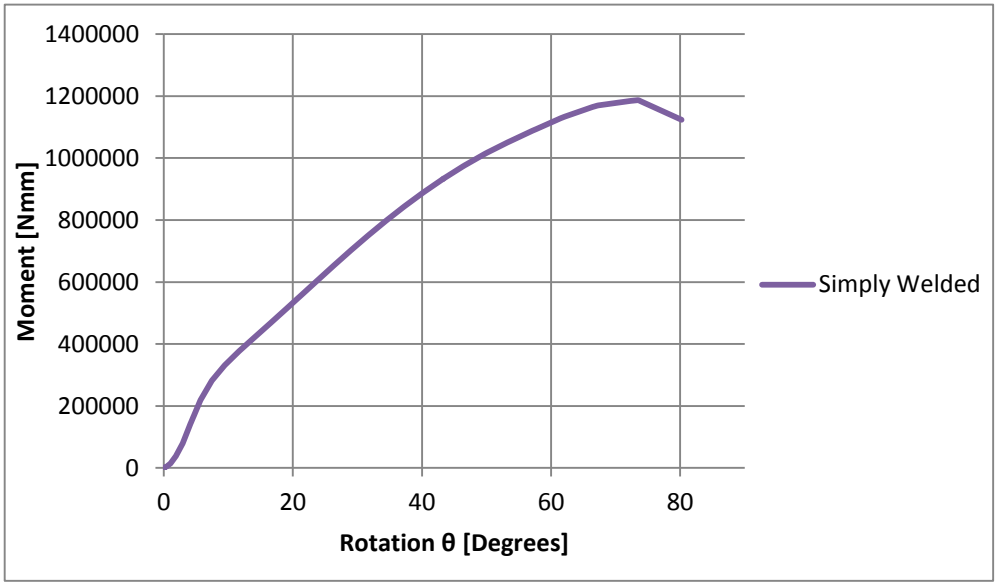

9-9. Moment-Rotation Curve. Configuration 2

On this configuration the maximum moment is close to 120000Nmm. But this maximum moment is achieved at an angle of more than 70 degrees which for practical cases it is not useful. Again, the first component to collapse is the floor (figure 9-10) and then the foot collapses (figure 9-11). Also, as C1, the tube does not collapse meaning that the foot and floor are not strong enough to produce tube collapse.

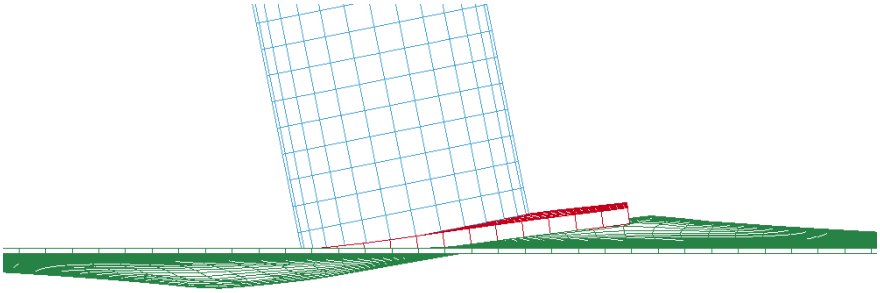

9-10. Floor Collapse. Configuration 2

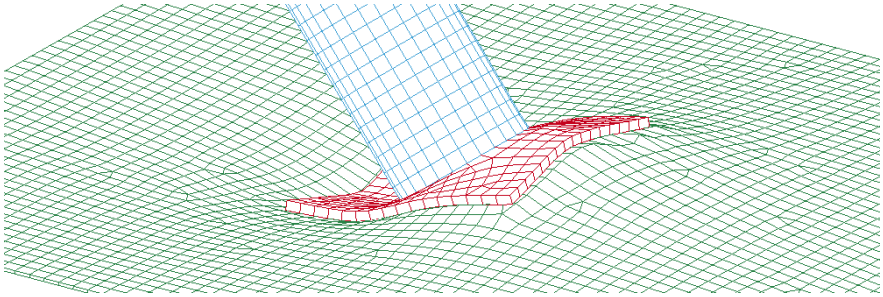

9-11. Foot Collapse. Configuration 2

9.5 Foot and Reinforcement Bolted (C3)

The configuration used for this model is using a reinforcement plate underneath the floor. All plates (foot, floor, reinforcement) are bolted together through the same holes. On the image below the FE model is presented.

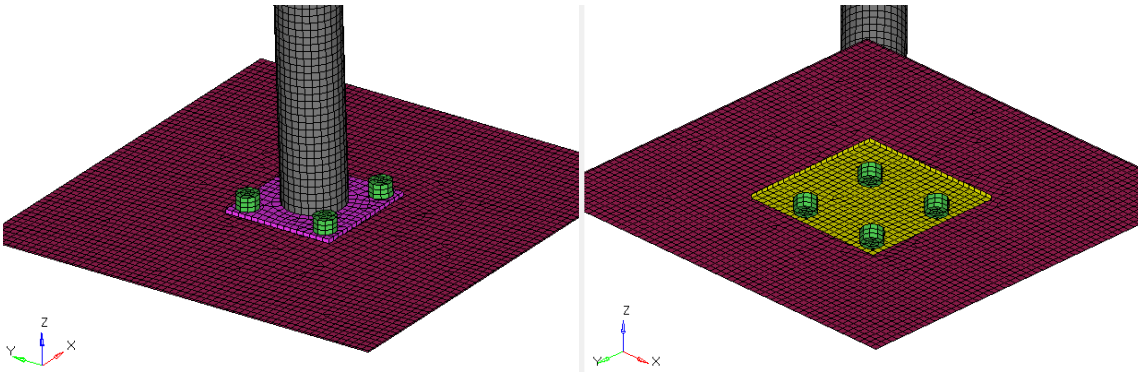

9-12. Bolted With Reinforcement FE Model

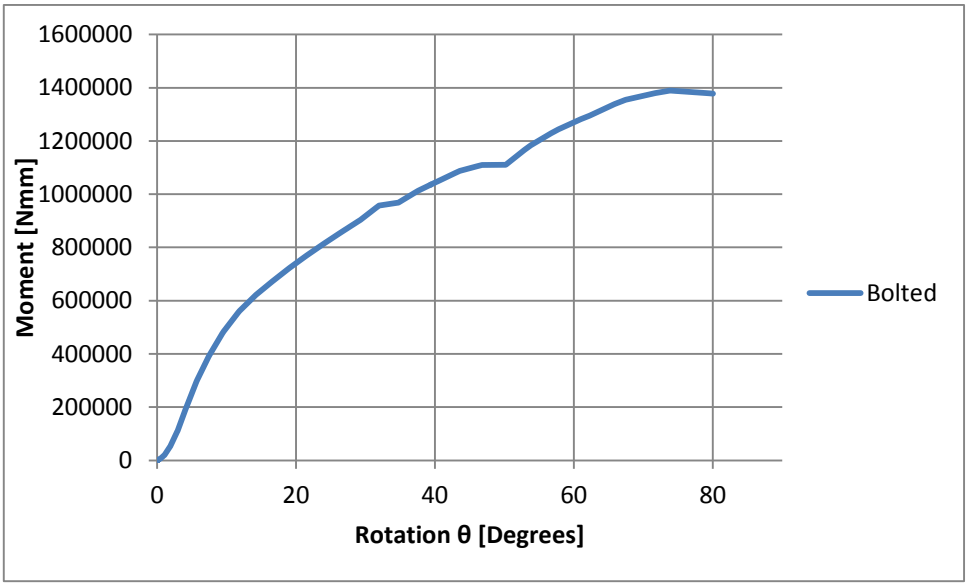

9-13. Moment-Rotation Curve. Configuration 3

At the sight of the moment rotation graph for this configuration, the maximum resisting moment is higher than the two previous but it is produced again in a very late stage regarding the rotation angle. Now, the reinforcement plays a role on the collapse mechanism and it is carefully analysed.

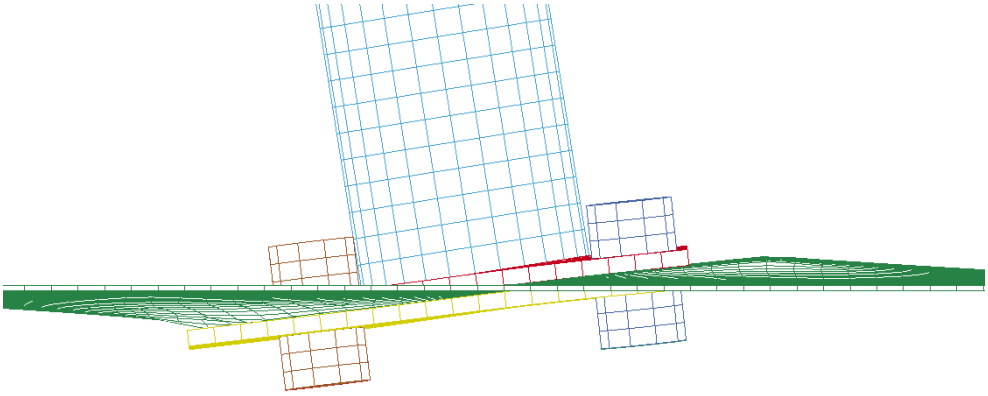

9-14. Floor Collapse. Configuration 3

On previous figure the floor collapse is presented. The reinforcement plate below pushes the floor upwards while the foot pushes the floor downwards producing and “S” shape on the floor. Again, as on all previous cases, the weakness of the floor produces a high rotation offering small resisting moment.

After floor collapses, foot and reinforcement plate start collapsing. Foot plate collapses in a similar shape as configuration 1. The reinforcement plate also

suffers deformation but it is clear that the addition of the reinforcement plate has strengthened substantially the mounting compared to C1.

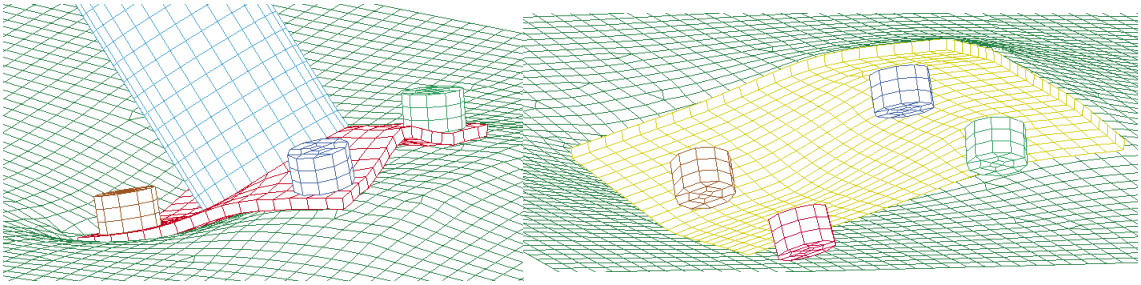

9-15. Foot and Reinforcement Collapse. Configuration 3

9.6 Foot Bolted and Reinforcement Welded (C4)

The last configuration considered includes a welded reinforcement to the floor on the top side. Then, the tube and foot part are bolted on top of the reinforcement. The configuration can be appreciated in the following figure of the model.

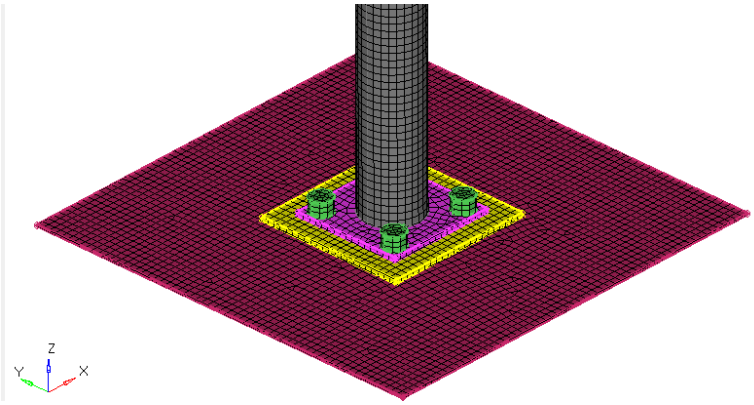

9-16. Bolted Foot With Welded Reinforcement FE Model

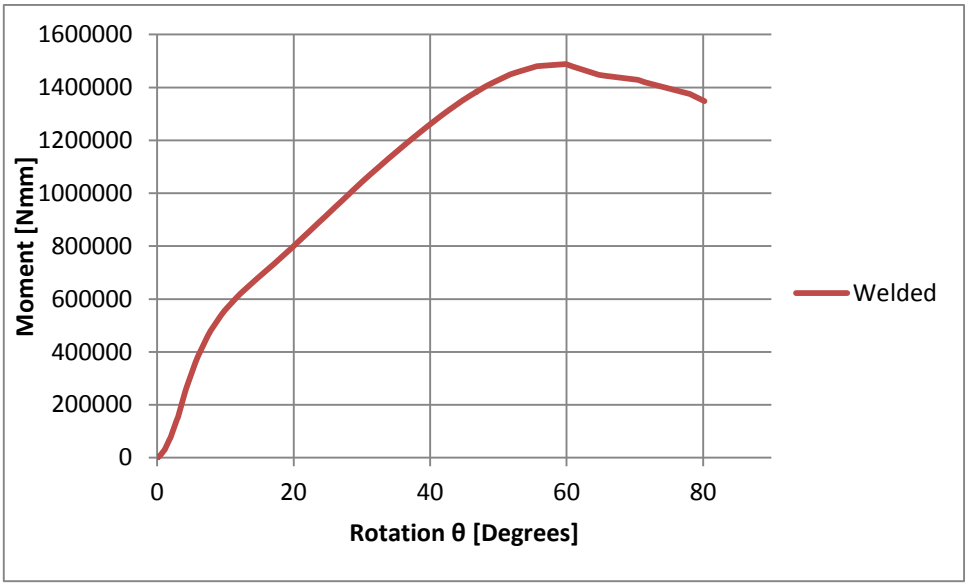

9-17. Moment-Rotation Curve. Configuration 4

The maximum resisting moment for this case is not much higher than C3 but what clearly changes is the angle where it occurs. This time the maximum moment angle is below 60 degrees which is a significant improvement from previous configurations where the angle is always around 80 degrees.

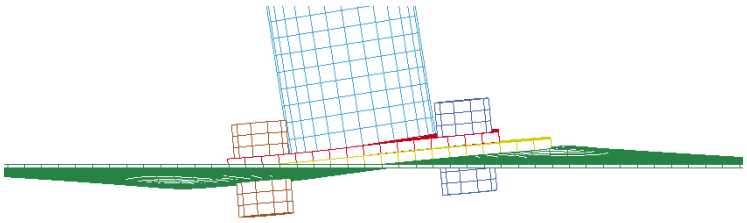

9-18. Floor Collapse. Configuration 4

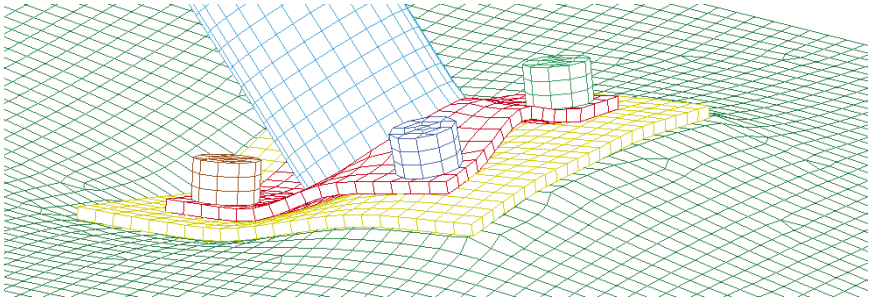

9-19. Foot Collapse. Configuration 4

Finally, observing deformed shapes of configuration 4, the welded reinforcement plate is pulling upwards the floor initially and on a second stage the foot starts collapsing. All four configurations presents similar deformed shapes with some particularities meaning that the difference of performance must be assessed using both deformed shape and strength curves.

From all previous results is concluded that the best design from all proposed is configuration 4, where a reinforcement plate is welded to the floor and foot plate bolted on top. Further parametric analysis will be performed on this configuration.

9.7 Moment-Rotation Curve Analysis

Moment-Rotation curve for configuration 4 is studied in more depth regarding the collapse modes at each section of the curves. Three different parts are clearly identified and they correspond to a different collapse mode of the mounting.

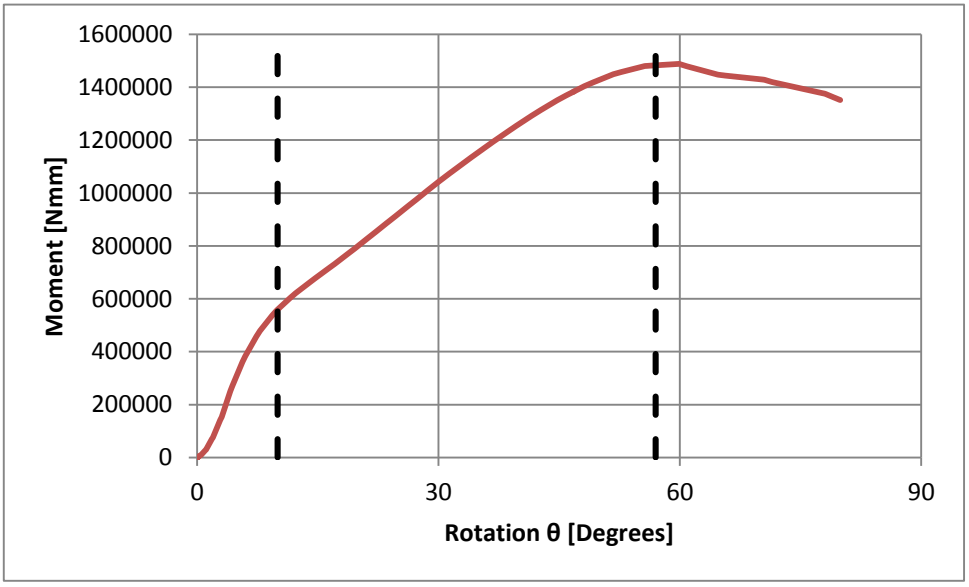

9-20. Moment-Rotation Curve Detailed Analysis

On previous graph, first section (from 0 to 10 rotation degrees) corresponds to floor collapse. From 10 to 57 degrees approximately foot is collapsing and from that point onwards the tube starts collapsing and therefore resisting moment starts to decrease.

10 EXPERIMENTAL RESULTS

10.1 Test Rig

To validate previous models test are performed. The configurations chosen for the test are C3 and C4 as they are the ones offering better performance.

Test rig used has a simple but effective operating mode. The specimen is clamped at one end and on the other end a winch is used to pull the tube on a fixed direction. On the following image a specimen fitted on the rig after test is performed is shown. Further detail of the rig and testing procedure are included in the Appendix section B.

10-1. Test Rig Set Up. After test image

Between the winch and the specimen a horse shoe dynamometer is fitter to measure the force applied. An LVDT device is attached to the tube to measure the displacement and use the readings to extract the tube rotation.

10.2 Test 1: Bolted

A first test is performed using C3 configuration provided by Safety Devices. The Rig, as it was constructed, only permitted a rotation of around 32 degrees of the tube, the limiting factor was the length of the LVDT. Moment rotation curves for experimental and simulation are compared up to 32 degrees of rotation.

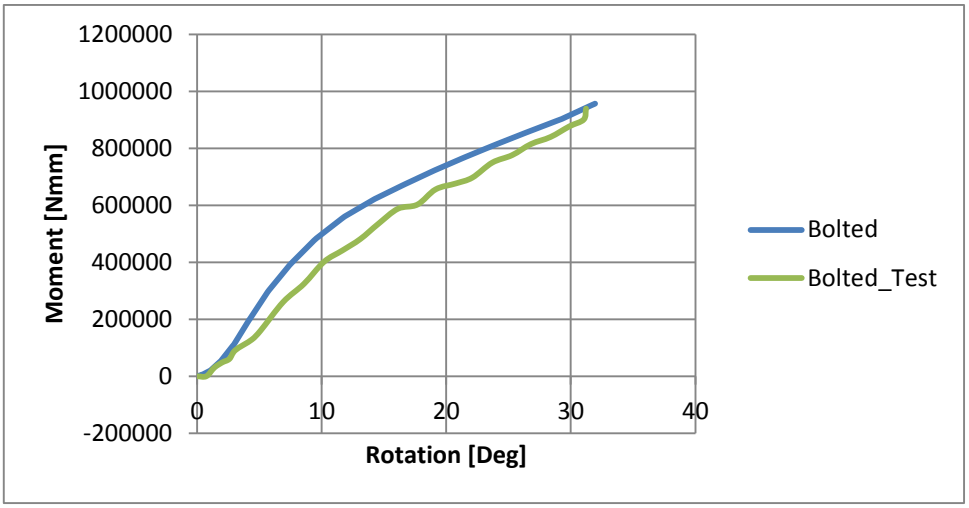

10-2. Moment-Rotation. Sim vs Test Bolted

The results obtained from both simulation and test are similar meaning that all the simulation approaches performed are acceptable. Some discrepancies though are observed being the highest error around 20%.

Regarding the collapse mode, the test agrees closely with the collapse shape on simulations. Initially, floor starts collapsing.

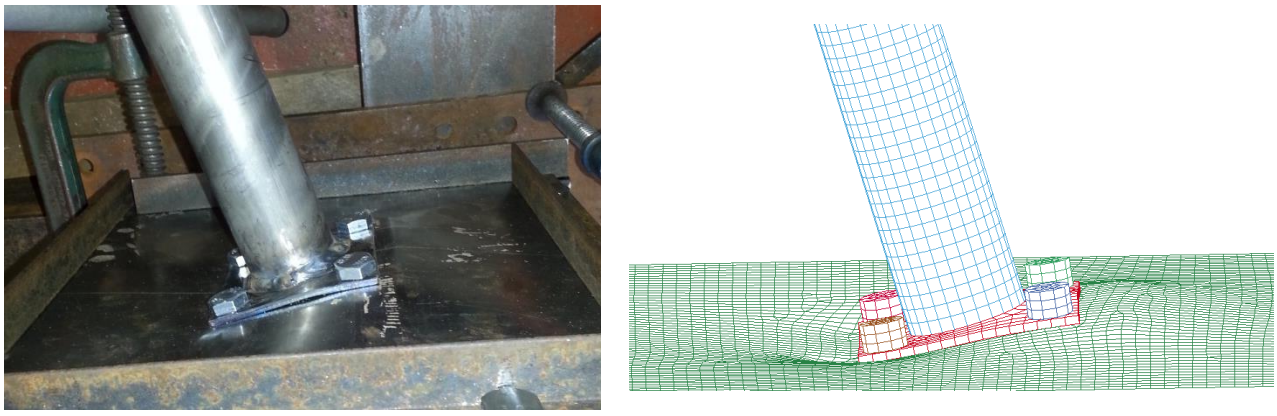

10-3. Floor Collapse. Test vs. Sim Bolted

On both cases, the floor is pulled up on tension site and pushed down on the compression side.

After floor is collapsed foot starts collapsing on both simulation and tests.

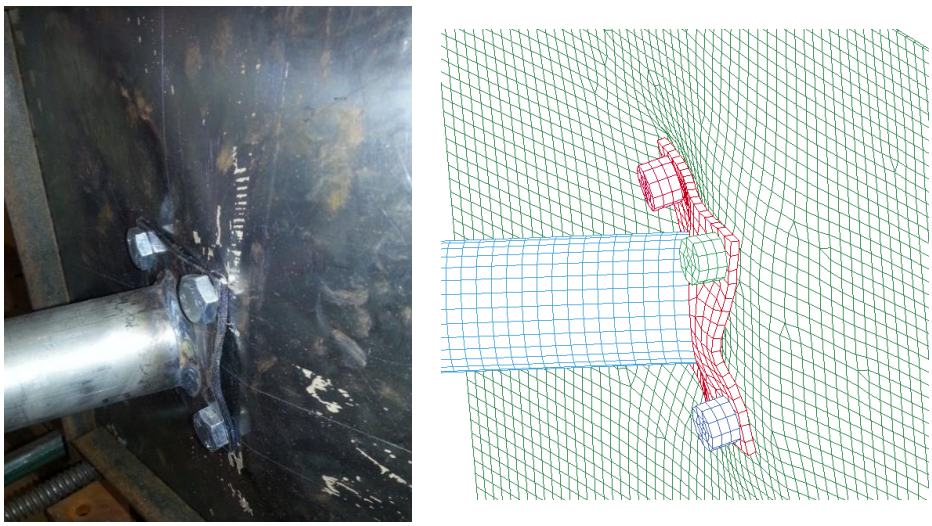

10-4. Foot Collapse. Test vs Sim Bolted

Similar deformed shape on test and simulation is observed when the floor is pulled up by the tube.

10.3 Test 2: Welded

The second test specimen is C4 where the reinforcement plate is bolted on top of the floor.

Moment-rotation curves comparison for test and simulation are the following.

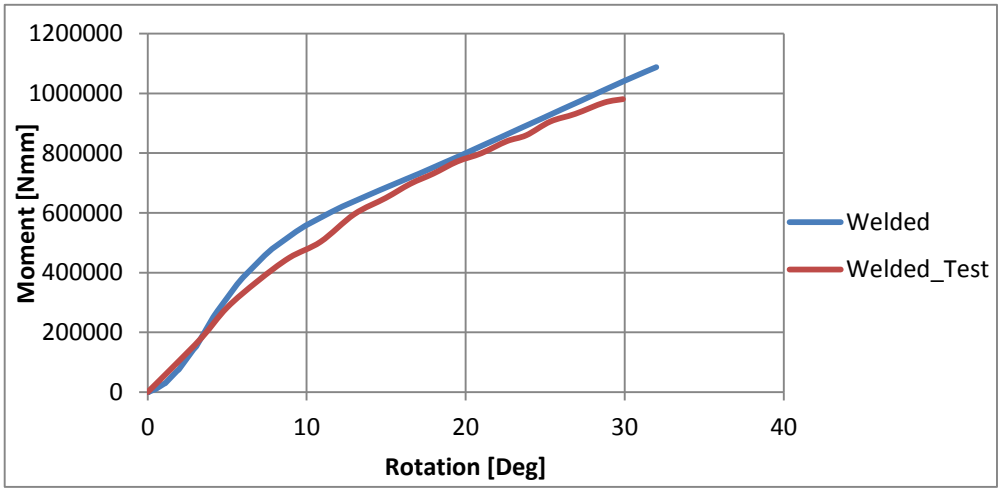

10-5. Moment-Rotation Curves. Test vs.Sim Welded

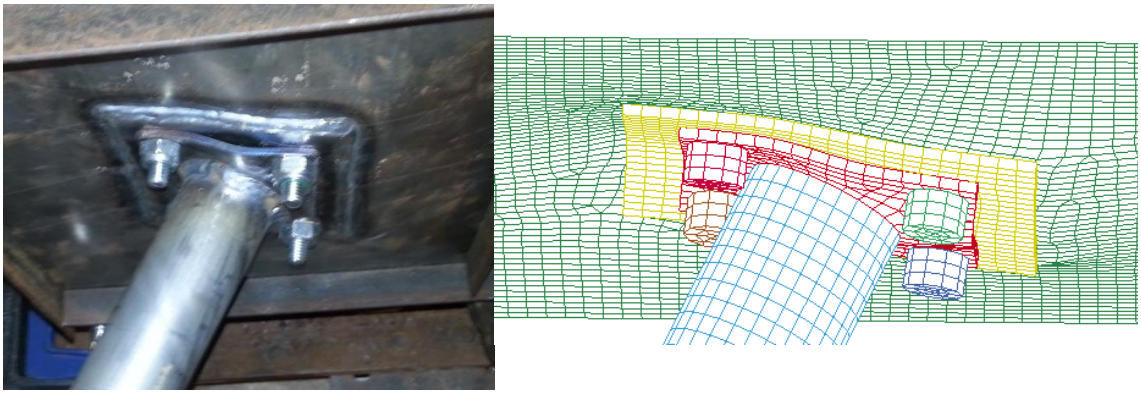

10-6.Floor Collapse. Test vs. Sim Welded

Similarly to previous test, floor starts collapsing and both simulation and test present similar behaviour.

At a certain rotation, as seen on C1 test, foot starts to lift and is pulled up presenting a good correlation regarding deformed shape between test and simulation.

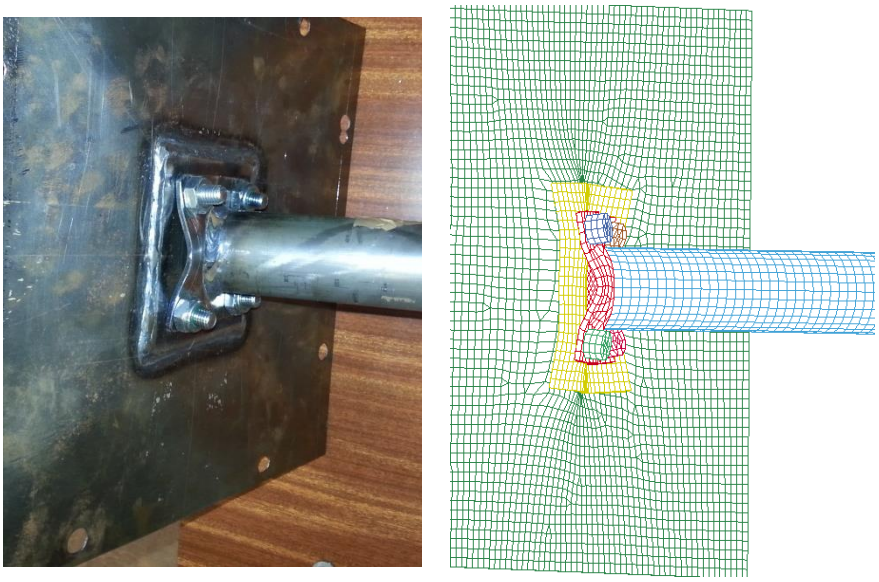

10-7. Foot Collapse. Test vs. Sim Welded

Finally, curves from both tests are plotted in the same graph.

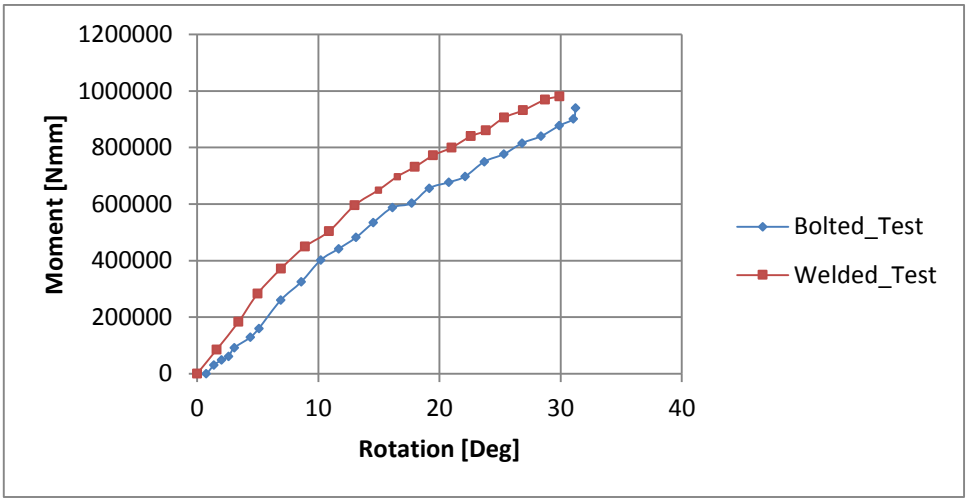

10-8. Moment-Rotation. Bolted and Welded Test

Welded curve lies above bolted specimen curve as it does on the simulation. With that result can be concluded that FE models achieve a good representation of the mountings tested.

11 PARAMETRIC ANALYSIS

Starting from C4 model, parameters floor size, foot thickness, reinforcement size are changed to assess the effect they have on the performance. On the following table the parameters used are presented.

Parameters	Values
Reinforcement size	100x100, 110x110, 120x120mm
Foot thickness	3, 4, 5, 6 mm
Floor size	220, 300mm

Table 11-1. Parametric Analysis Resume Table

Curves for each parameter are plotted on the same graph and the behaviour of the mounting is assessed.

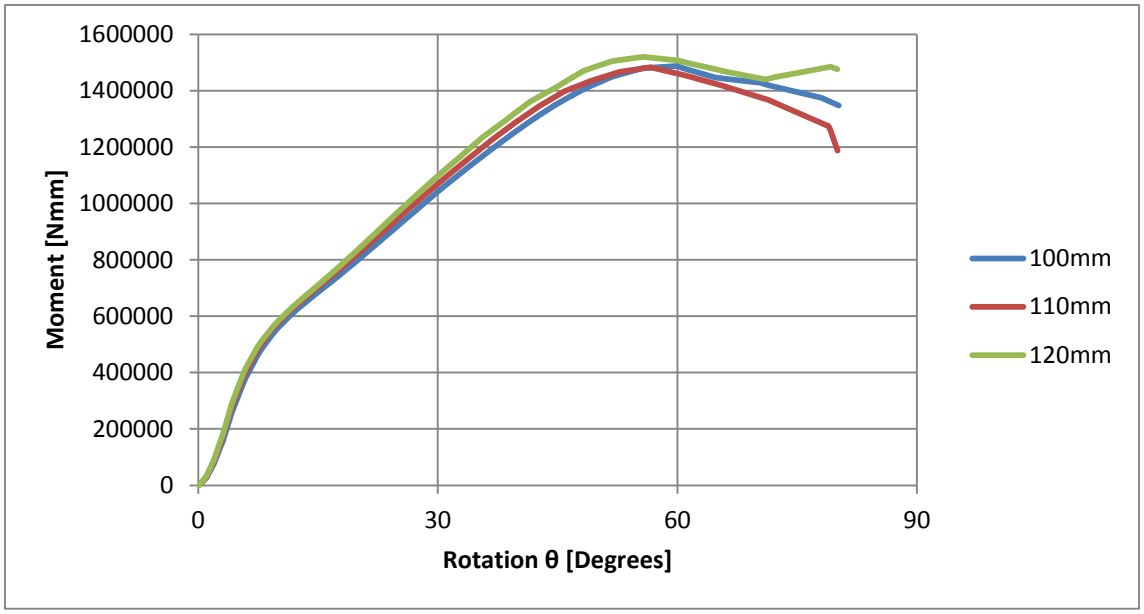

11-1. Parametric Analysis. Reinforcement size

At the sight of the previous results, reinforcement size has a minimum effect on the strength. Maximum resisting moment rises less than 5% changing the size from 100x100 to 120x120.

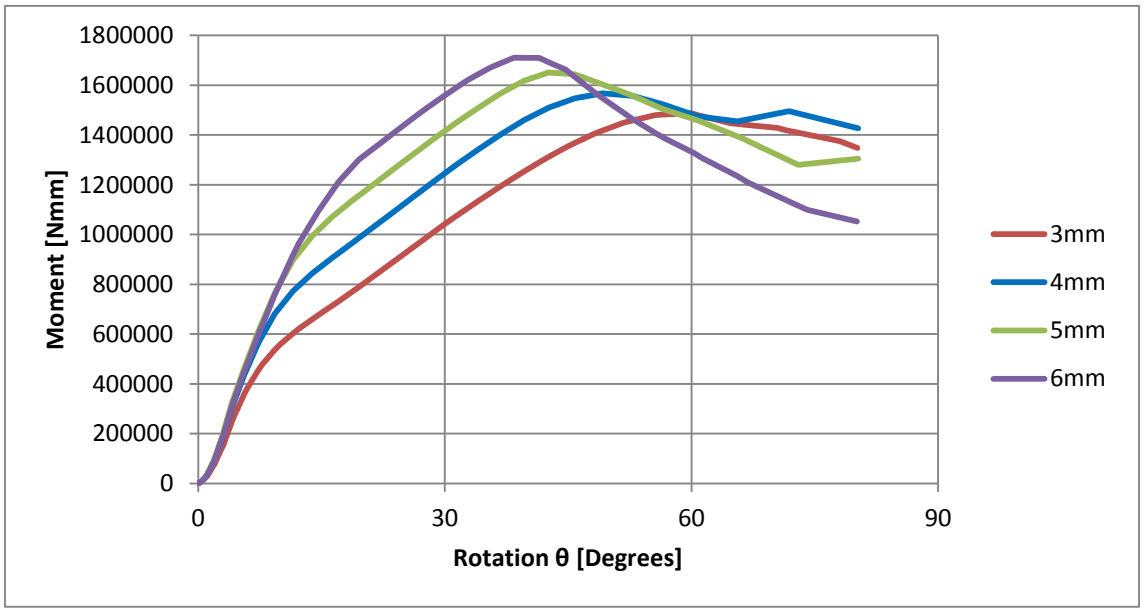

11-2. Parametric Analysis. Foot thickness

Regarding foot thickness, the effect of this parameter to mounting performance is considerable. Using 3mm foot thickness maximum resisting moment achieves a value close to 1,5 kNm at around 60 degrees. When increasing the thickness

to 6mm this maximum value raises up to 1,75kNm at a rotation angle around 35 degrees.

Finally, to check if the floor size has any influence on the performance two floor dimensions are simulated.

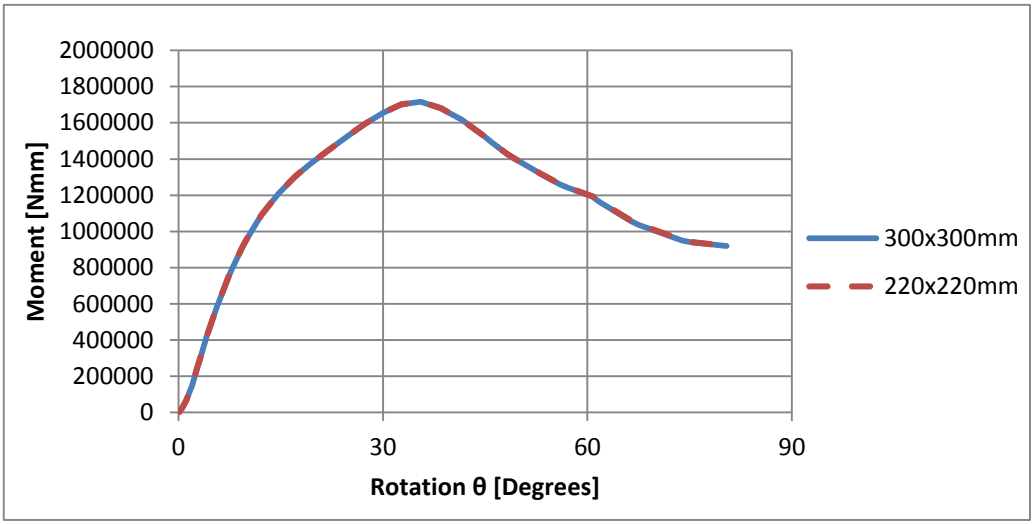

11-3. Parametric Analysis. Floor size

No influence is observed regarding floor size. This analysis is performed to check if whether the proximity of constrained edges of the floor to the mounting are over-stiffening the design or not.

12 DISCUSSION AND CONCLUSIONS

12.1 Discussion

Using both simulation and test method it was observed that a critical parameter regarding foot mounting of roll cages to vehicle frames is the foot thickness. The ideal thickness for this plate is concluded to be higher than 6mm which is not a common plate thickness on the industry that uses 3mm thick plates.

Floor plate is a component affecting considerably the performance of the mounting but it is fixed by vehicle manufacturers and not by roll cage industry. On FIA test, the softness of those components is not detected as floor plate is not included on the specimen test and foot of the roll cage is rigidly fixed. With that configuration an over-stiffening of the cage is produced which results in a poor behaviour when fitted into the car when compared with test strength of the roll cage.

Including reinforcement improves significantly the performance of the mounting. Studied configurations without reinforcement offered a poor performance and therefore those configurations are not studied in depth in this work. Configurations without reinforcement should not be used for roll cages attachments and, although configurations without reinforcement are suggested to study by the company, it is actually a generalised practice to include reinforcements.

12.2 Conclusions

- Foot thickness is the parameter affecting the most on mounting performance.
- Floor reduces considerably roll cage performance as it is weakest component of the mounting.
- FIA test is not representative, floor should be included.
- Reinforcement size affects mounting performance not as much as foot thickness.
- Combinations of foot thickness and reinforcement size can be used to improve the performance, being foot thickness the most important parameter.

13 FUTURE WORK

- Include preload on all mounting models.
- Repeat test allowing more angle of rotation
- Perform test using 6 mm thick foot.
- Perform FIA test simulation on a roll cage model with foot and floor
- Perform material characterisation tests (tensile, three point bending) on Safety Devices specimen' material to introduce more accurate material parameters on the FE models.

14 REFERENCES

[1] W. Deutermann, National Highway Traffic Safety Administration (NHTSA), (April 2002) ‘‘Characteristics of fatal rollover crashes’’, National Centre for Statistics and Analysis Research and Development, Washington D.C

[2] Safety Devices Ltd. Images Gallery, Available at: www.safetydevices.com, Accessed: 1st June 2014.

[3] World Auto Steel, Steel Market Development Institute (May 2011) “Future Steel Vehicle”, Available at: www.autosteel.org Accessed: 25th July 2014.

[4] FIA Technical regulations (2013), Article 253, appendix J. Available: http://www.fia.com/sites/default/files/regulation/file/253%20(2013).pdf accessed: 16th May 2014.

[5] Safety Devices Ltd., Technical roll cage information. Available at: http://www.safetydevices.com/motorsport/technical/ Accessed: 20th May 2014.

[6] G. L. Kulak, J. W. Fisher, J. H. A. Smith (2001) “Guide to Design Criteria for Bolted and Riveted Joints”, Second Edition, American Institute of Steel Construction, United States.

[7] LS-DYNA Examples, Contact. Available at: http://www.dynaexamples.com/intro-by-k.-weimar/contact Accessed: 22nd May 2014

[8] S. Narkhede, N. Lokhande, B. Gangani, G. Gadek, ‘’Bolted Joint Representation in LS-DYNA to Model Bolt Pre-Stress and Bolt Failure Characteristics in Crash Simulations’’, 11th International LS-DYNA Users Conference, Miami, USA - June 6-8, 2010

[9] F. Godillon, ‘’Crashworthiness Study of a Rally Car Safety Cage’’ MSc Thesis, Cranfield University, September 2002

[10] S.Poonaya, U.Teebonma, C. Thinvongpituk, ‘’Plastic Collapse Analysis of Thin-walled Circular Tubes Subjected to Bending’’, Thin Walled Structures, vol.47, pg. 637-645.

[11] Livermore Software Technology Coorporation, “LS-DYNA Keyword User’s Manual”, Volume I, Version 971, April 2012

[12] D. Ball, “ Rear Impact Crashworthiness of Triangulated Space Frame Sports Cars”, MSc Thesis, Cranfield University, August 2008.

[13] J. C. Brown, Introduction to Crash Energy Management, Cranfield University Crashworthines Lecture Notes, 2011.

APPENDICES

Appendix A

A.1 Mountings Parts

Mounting configurations used on this work are assembled using three components. Separate components are the following: Foot plate&Tube, Reinforcement and Floor. Dimensions of those components are presented below on the drawings for each configuration.

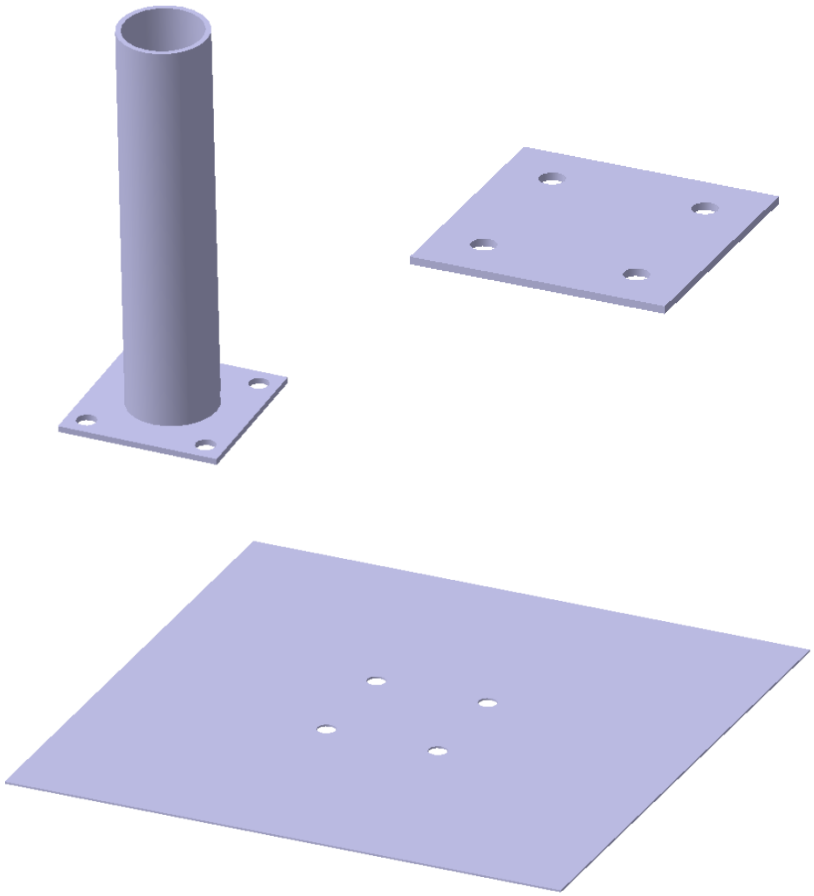

14-1.Mounting Components CAD parts

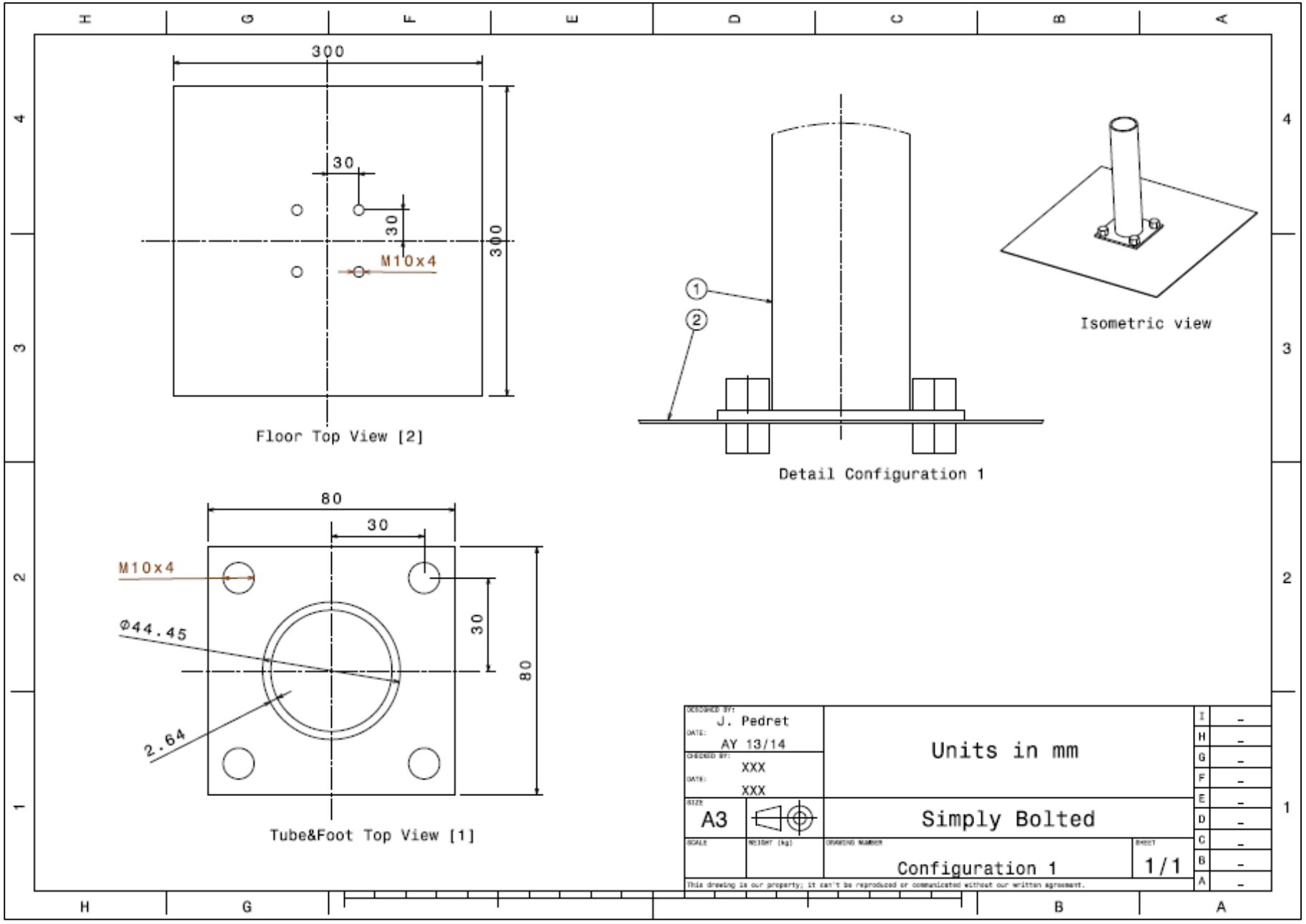
300
30
30
300
M10x4
Floor Top View [2]
1
2
Detail Configuration 1
Isometric view
80
30
M10x4
Φ44.45
30
80
2.64
Tube&Foot Top View [1]
DESIGNED BY: J. Pedret
DATE: AY 13/14
CHECKED BY: XXX
DATE: XXX
SIZE A3
SCALE
WEIGHT (kg)
DRAWING NUMBER Configuration 1
SHEET 1/1
Units in mm
Simply Bolted
This drawing is our property; it can't be reproduced or communicated without our written agreement.
I -
H -
G -
F -
E -
D -
C -
B -
A -

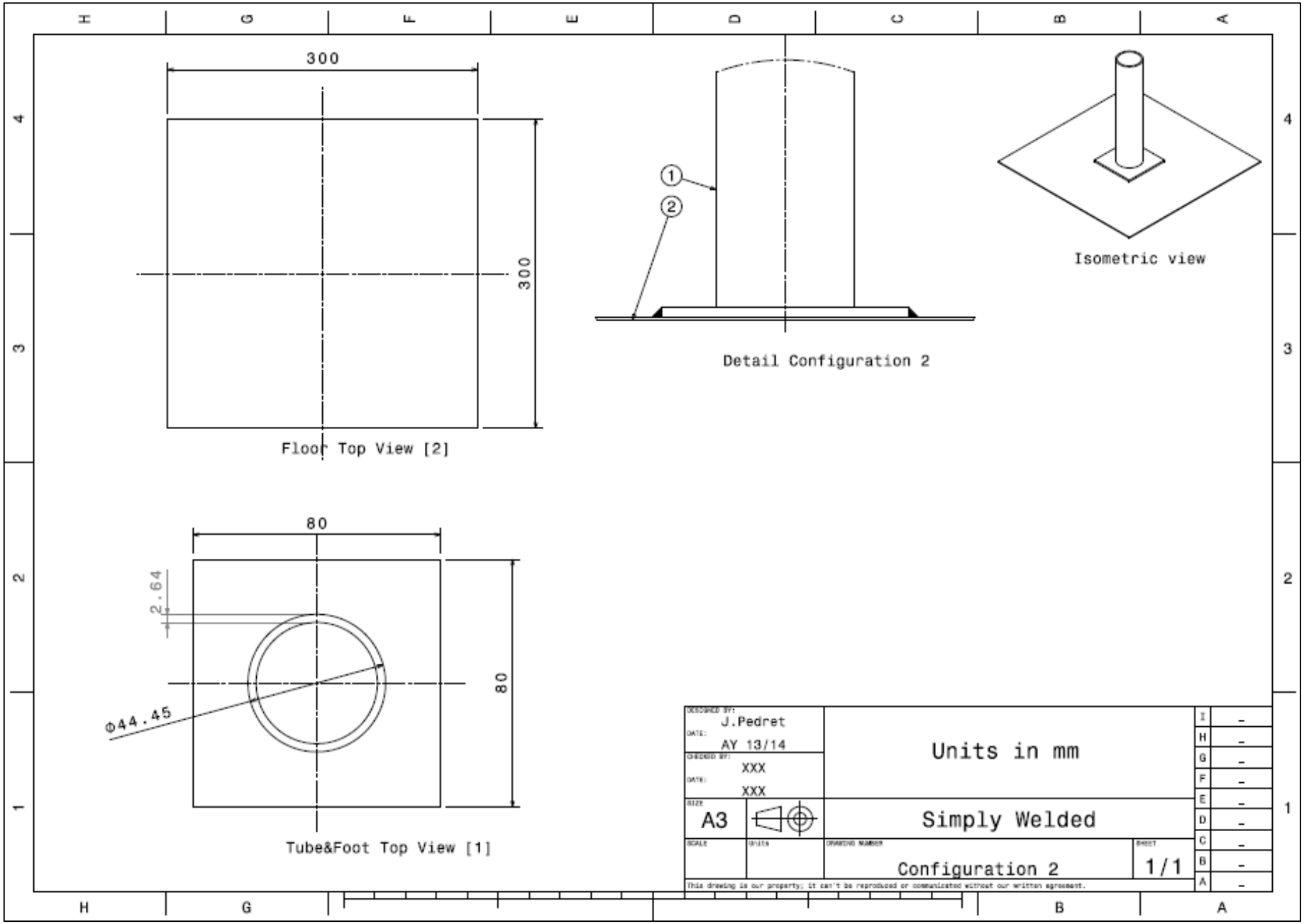
300
300
Floor Top View [2]
1
2
Detail Configuration 2
Isometric view
80
2.64
80
Φ44.45
Tube&Foot Top View [1]
DESIGNED BY: J.Pedret
DATE: AY 13/14
CHECKED BY: XXX
DATE: XXX
SIZE A3
SCALE
UNITS
Units in mm
Simply Welded
DRAWING NUMBER Configuration 2
SHEET 1/1
This drawing is our property; it can't be reproduced or communicated without our written agreement.
I -
H -
G -
F -
E -
D -
C -
B -
A -

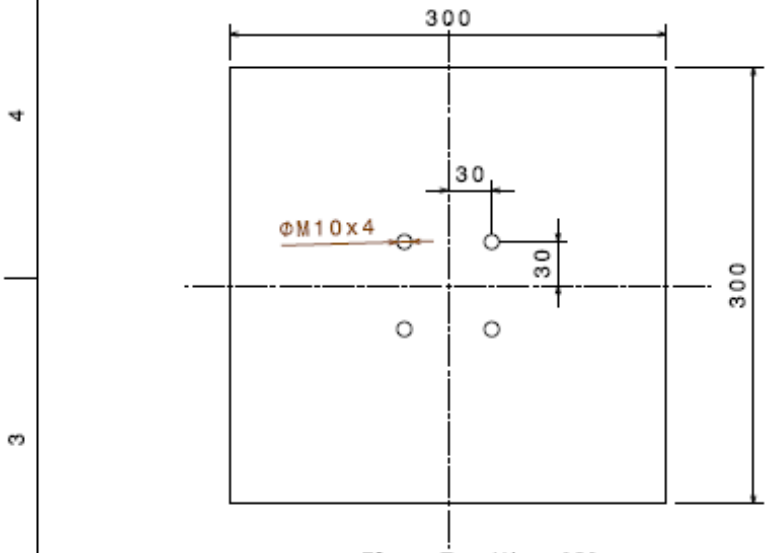

Floor Top View [2]

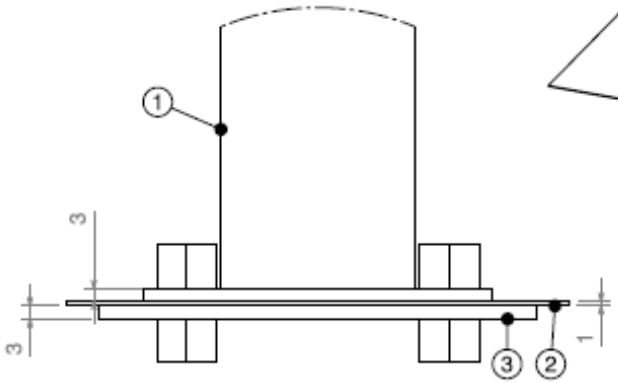

Detail Configuration 3

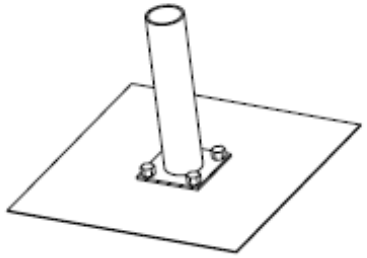

Isometric view

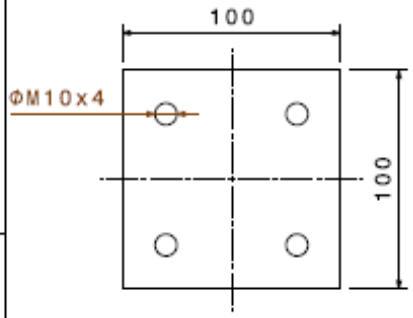

Reinforcement Top View [3]

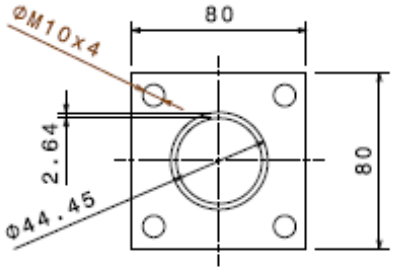

Tube&Foot Top View [1]

DESIGNED BY: J.Pedret		Units in mm	I –
DATE: AY 13/14			H –
CHECKED BY: XXX			G –
DATE: XXX			F –
SIZE A3		Bolted	E –
			D –
SCALE	WEIGHT (kg)	DRAWING NUMBER Configuration 3	SHEET 1/1 C –
			B –
This drawing is our property; it can't be reproduced or communicated without our written agreement.			A –

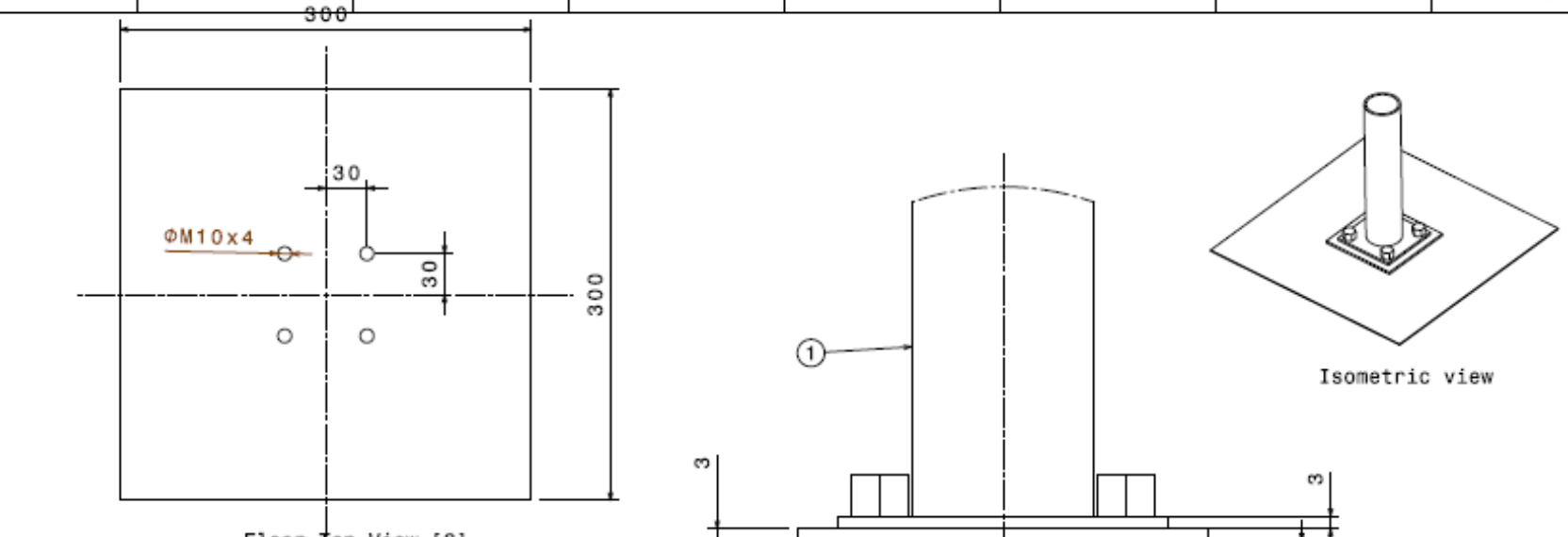

Floor Top View [2]

Detail Configuration 4

Isometric view

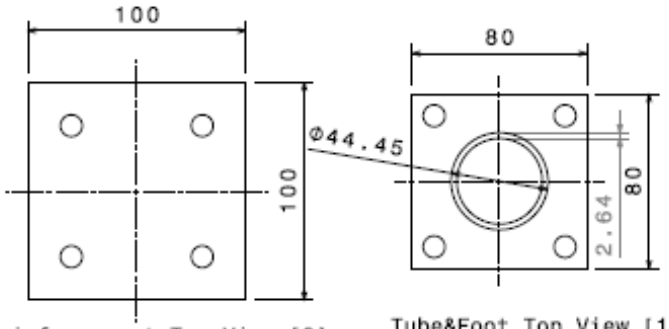

Reinforcement Top View [3]

Tube&Foot Top View [1]

DESIGNED BY: J.Pedret		Units in mm	
DATE: AY 13/14			
CHECKED BY: XXX			
DATE: XXX			
SIZE A3		Welded	
SCALE	WEIGHT (kg)	DRAWING NUMBER Configuration 4	SHEET 1/1

I	-
H	-
G	-
F	-
E	-
D	-
C	-
B	-
A	-

Appendix B

B.1 Test Rig

Test rig used for this project is designed from a previous rig available on Cranfield University Lab.

The existent rig was used to clamp circular tubes on its base to perform a bending test. For this project, as explained on section 4 and appendix section A, the tubes are attached to a metal plate, and this plate must be clamped and not the tube. The data reading and force application devices follow the same approach of the previous work rig. All connections used will be explained precisely to permit repeatability of the experiments in the future.

The aspect of the rig is the following.

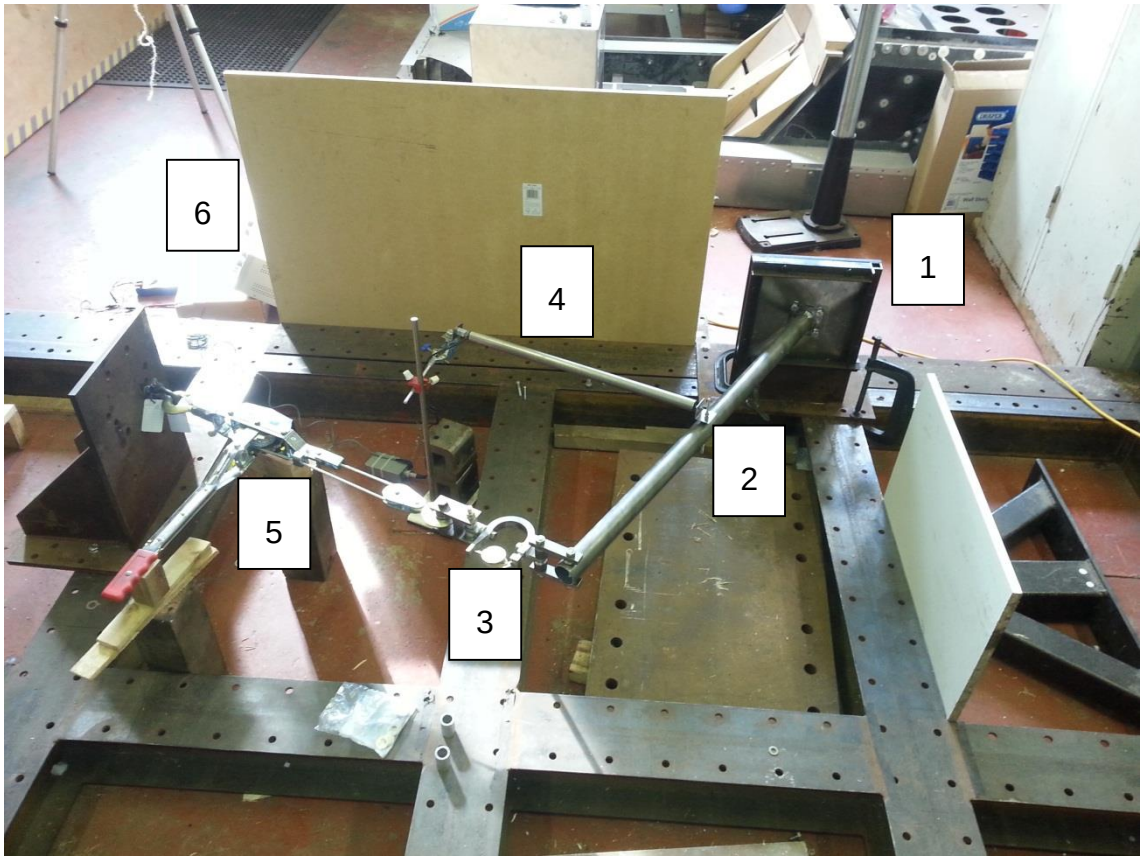

14-2. Test Rig Configuration. After test capture

Where:

1. **Clamping system**. The specimen is clamped to a horizontal bracket using a simple clamping system, presented below.

   Square tubes are situated below the specimen and sheet metals plates are positioned on top of the specimen. All components are then bolted together to the lab's bracket and the specimen is therefore clamped.

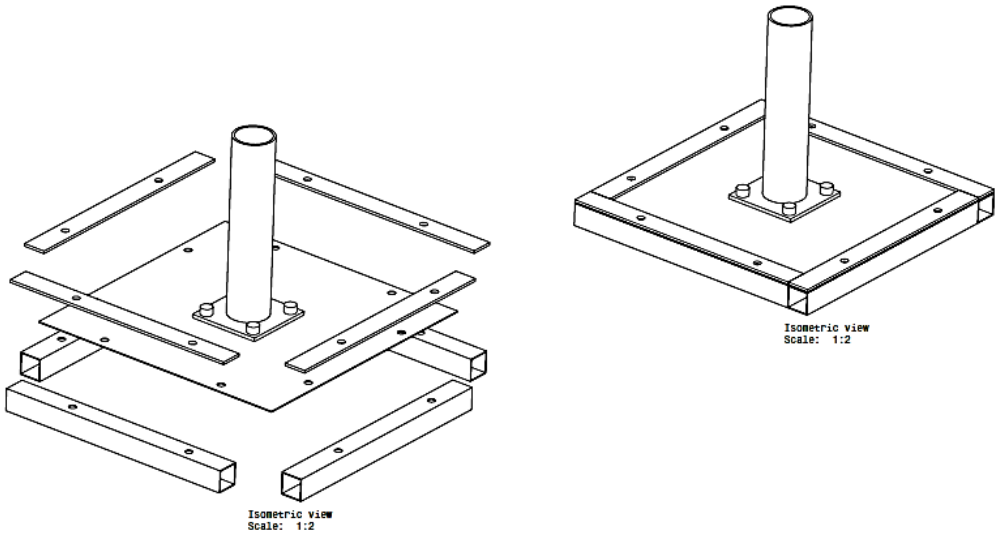

14-3. Clamping System. Drawing

14-4. Clamping System. Actual Rig

2. Specimen.

   Two specimens are used for this work, C3 and C4. See Appendix section A for configurations detail.

3. **HorseShoe Dynamometer.** A horseshoe dynamometer is a force measure device available at Cranfield University Lab. The working principle is simple. An U shape metal is placed on some point where the force is applied. The connections must be placed at the ends of the U. When force is applied, those ends tend to separate and that displacement is measured with a pointer indicator (see figure below).

   Before the test, the device must be calibrated using a tensile test machine. In this case, the load limit of the cell is 5kN and therefore is used in a 5kN tensile machine to use all the operating range and reduce the error.

   Increments of 100 N are applied to the load cell and the divisions progress on the pointer are registered. Then a curve is fitted and the force-division parameter is extracted.

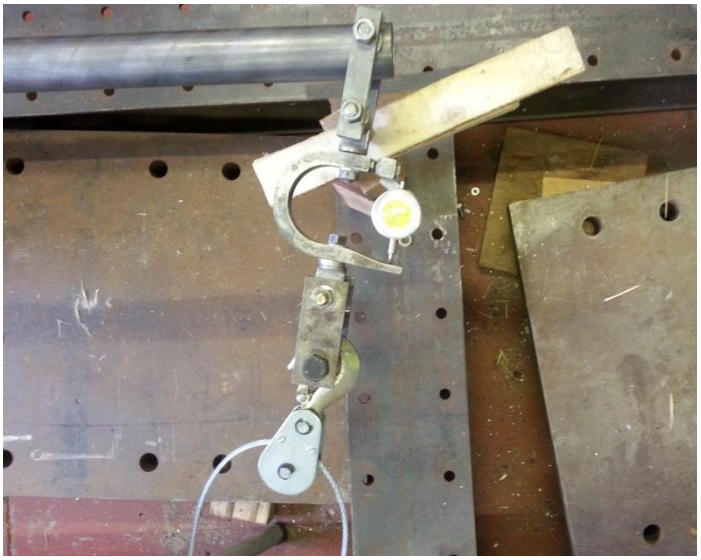

14-5**. HorseShoe Dynamometer. On test rig**

4. LVDT. A linear variable differential transformer is an electrical transformed used to measure linear displacements. Given an input voltage, when the metal moveable bar is displaced, and output voltage changes due to

transformers inside the device. This apparatus also needs calibration before the test to obtain the displacement-voltage parameter.

5. **Ratchet Winch**. A ratchet winch is a machine typically used for industrial purposes. In this case is used to apply the force on the test, which is not its usual function but it can do the job for the present work.

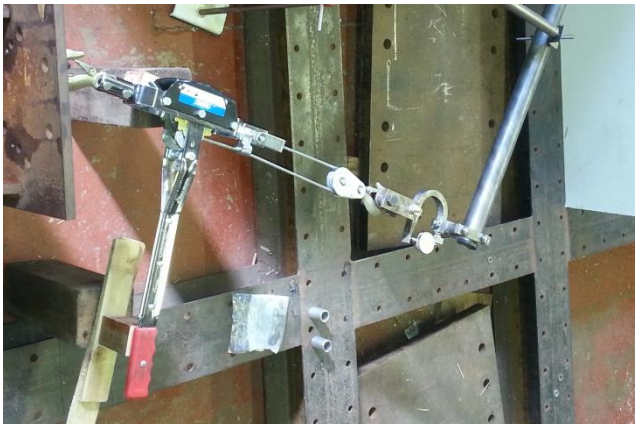

14-6. Ratchet Winch. On test rig

6. **Power Supply and Voltmeter**. Finally, a power supply and voltmeter are used. Power supply system is needed to provide a constant voltage to the LVDT device as input and voltmeter is used to read the output voltage of the LVDT.

B.1.1 Load cell calibration

As mentioned, horse shoe dynamometer needs prior calibration to obtain accurate test readings. Methodology followed to calibrate the device consists on applying a known force to the dynamometer using a tensile test machine. Two test are performed applying force with increments of approximately 100N. At each force increment the readings on the pointer indicator are registered. Plotting those force-division values on a graph and obtaining the linear regression parameters the result is the following.

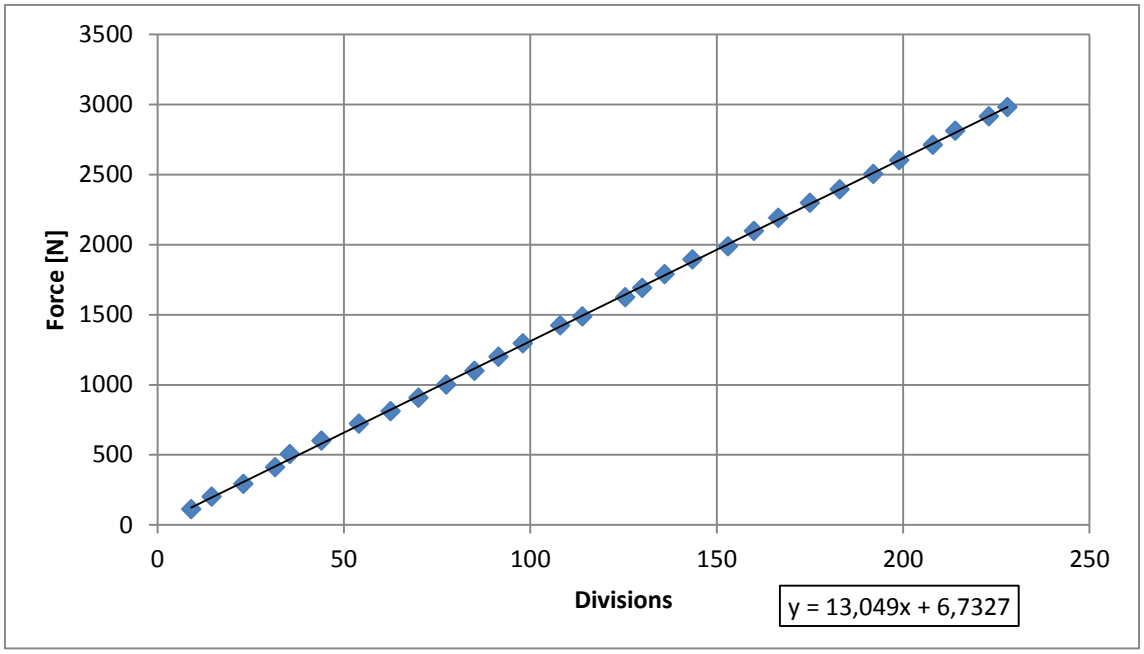

14-7. Dynamometer Calibration

Obtaining a factor for the Dynamometer of 13.049 N/Div.

B.1.2 LVDT Calibration

For the same reason as the load cell, the device measuring the displacement must be also calibrated. In this case, two readings are performed. One of them is obtained when extending the device and the other when contracting the moving part of the device.

Graphs for the calibration with respective regression lines are the following.

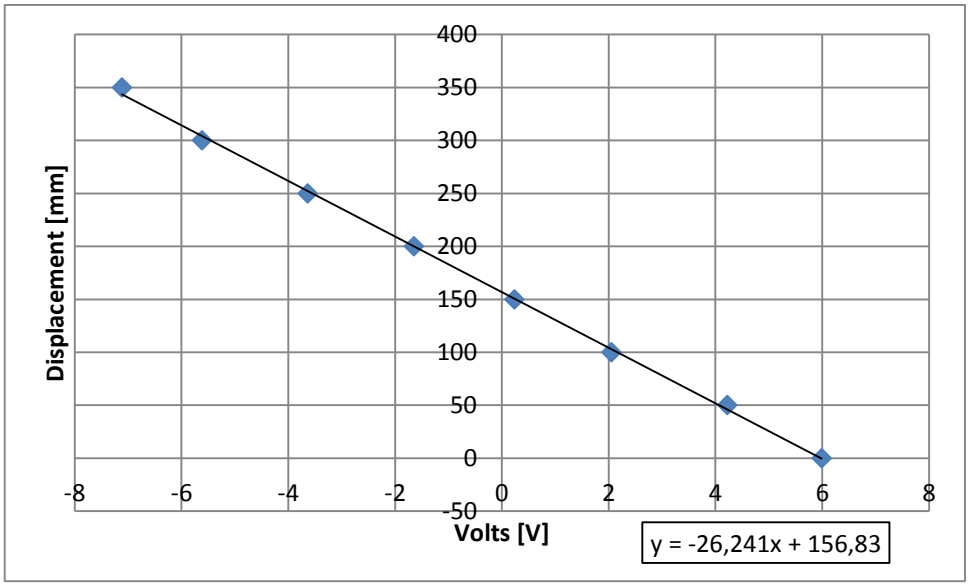

14-8. Reading 1. LVDT Calibration

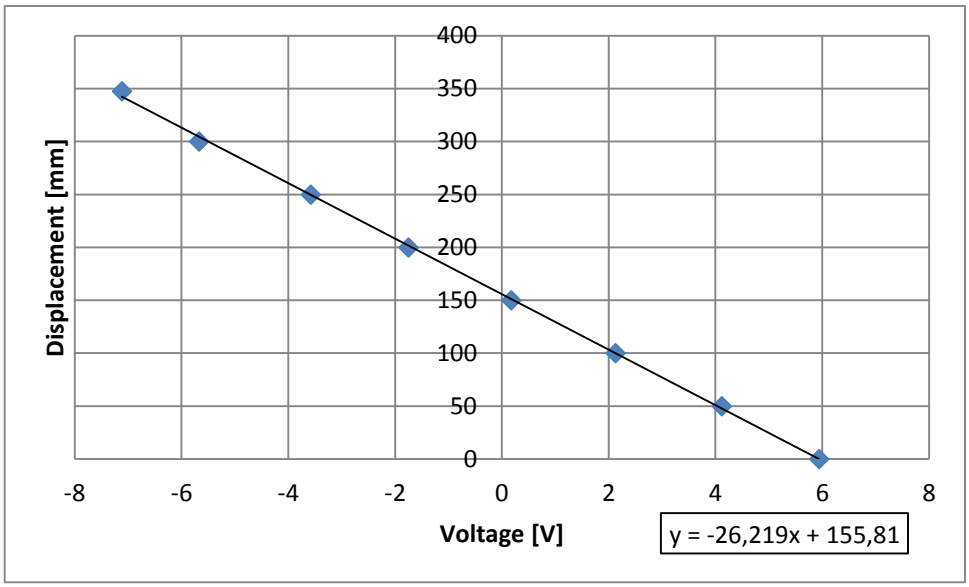

14-9. Reading 2. LVDT Calibration

Mean value of both reading is used to obtain test results. LVDT factor used is -23.23mm/V.

B.2 Test Procedure

Perform the actual test is a quick step of the work. The only procedure followed is to apply force using the ratchet winch and record the readings on both voltmeter and horseshoe dynamometer every 50Volts.

Mainly, the steps followed during the test once the specimen is set up in the initial position are the following:

1. Check LVDT reading and register the value.
2. Check Dynamometer reading and, if not zero, adjust the pointer so the initial value registered is zero.
3. Apply increments of displacement using the ratchet winch until an increment of 50V is observed on the voltmeter.
4. Check LVDT and Dynamometer register their readings.
5. Repeat steps 3 and 4 until moving part of the LVDT reaches its limit.

B.3 Test Moment-Rotation curves. Formulae

From test, data obtained is the couple of values volts (from LVDT) and corresponding divisions (from dynamometer). Knowing then initial positions of certain points of the test rig and specimen, the final curve moment rotation can be derived.

As previous projects have been carried using same rig configuration a spreadsheet is used to perform such transformations. The following pages explain how geometrical transformations are derived in order to obtain final moment rotation curves. Information is fully extracted from D. Ball [12] MSc thesis. Student thesis involver rear crash study of triangulated frame of sports car and tube were tested in a similar manner as the current project.

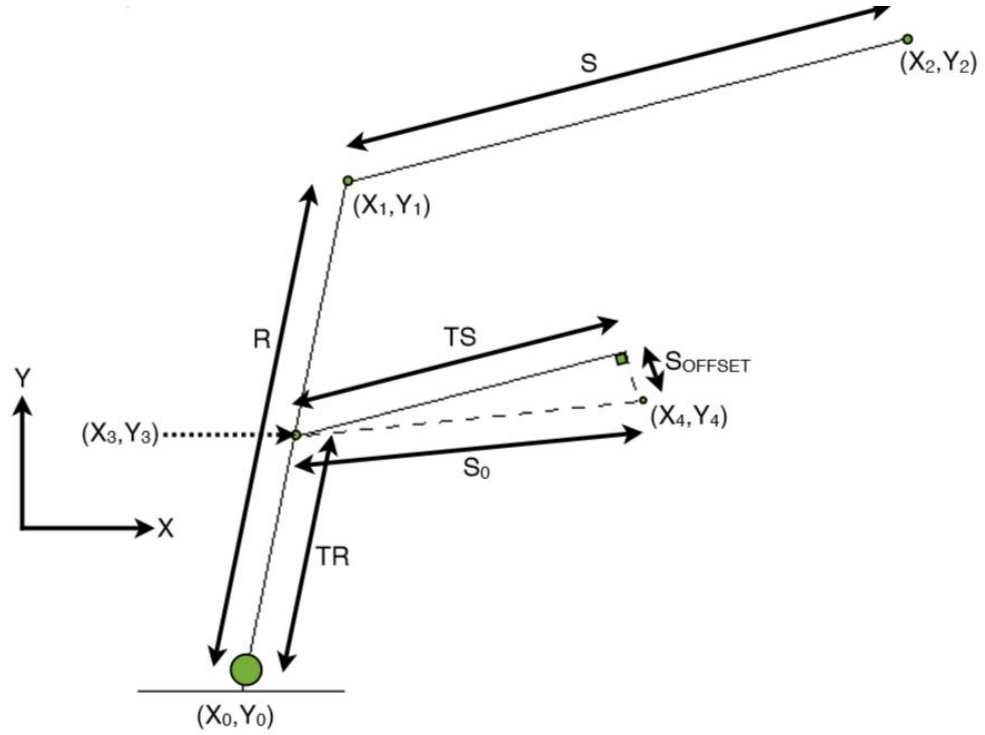

S	Length of winch from floor mount to tube mount; S_0 at initial pos.
R	Length of sample from plastic hinge to tube mount
S_{offset}	Offset distance between LVDT pivot and line of action (equals 0)
S_0	Distance between centre of ball joint and LVDT pivot at the beginning
TR	Length of sample between plastic hinge and centre of ball joint
(X_0,Y_0)	Location of plastic hinge
(X_1,Y_1)	Location of tube mount
(X_2,Y_2)	Location of winch mounting point
(X_3,Y_3)	Location of ball joint
(X_4,Y_4)	Location of LVDT pivot
V_1	LVDT Reading. V_{10} at beginning
V_2	Dynamometer reading; V_{20} at beginning
K_1	Calibration factor of LVDT

K_2 Calibration factor of dynamometer

TS Length of LVDT. TS_0 at beginning $=SQRT(S_0^2+S_{offset}^2)$

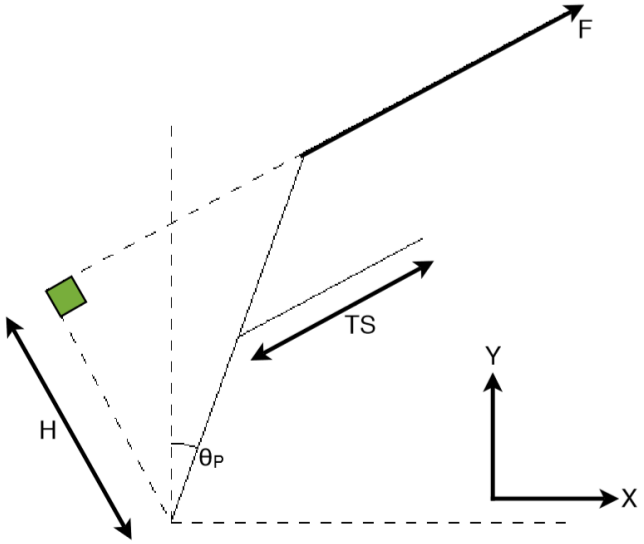

H Moment arm length

Θ_p Plastic hinge rotation

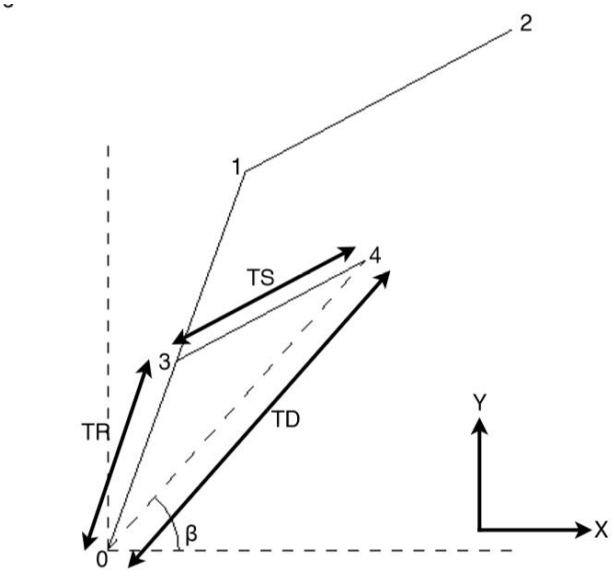

ΔT $=TS-K_1 \cdot (V_{10}-V_1)$

ΔTS $=TS_0-\Delta T$

TR^2 $=(X_3-X_0)^2+(Y_3-Y_0)^2$

TD^2 $=(X_4-X_0)^2+(Y_4-Y_0)^2$

β $=\tan^{-1}(Y_4/X_4)$

Alternate axis (q,p):

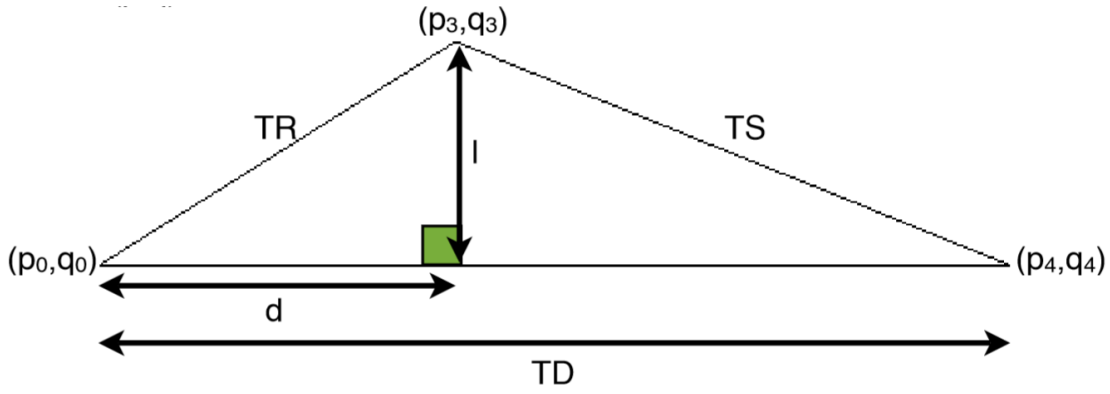

p_3 $=d$

q_3 $=l$

TR^2 $=d^2+l^2$

TS^2 $=(TD-d)^2+l^2$

TS^2-TR^2 $=TD^2-2TDd+0$

d $=[TD^2-TS^2+TR^2]/[2TD]$

l $=SQRT(TR^2-d^2)$

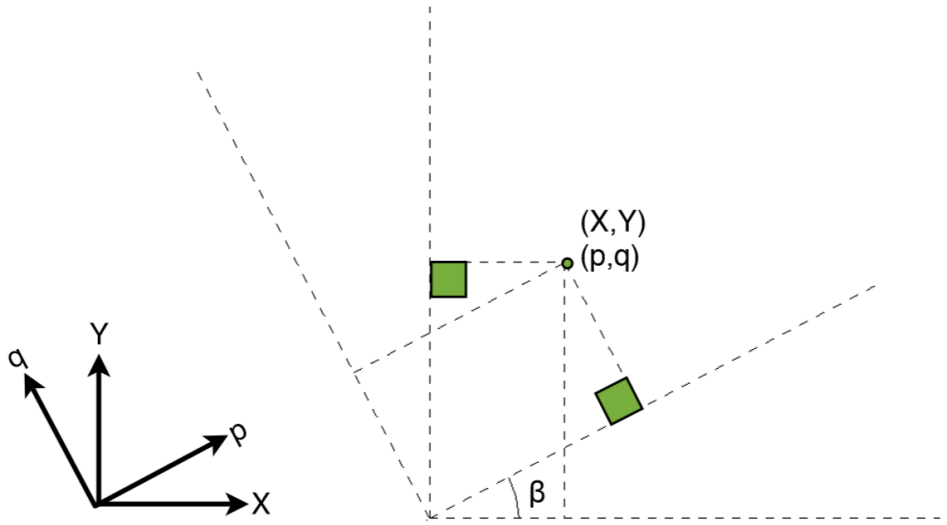

X_3 $= p_3 \cos \beta - q_3 \sin \beta = d \cos \beta - l \sin \beta$

Y_3 $= p_3 \sin \beta + q_3 \cos \beta = d \sin \beta + l \cos \beta$

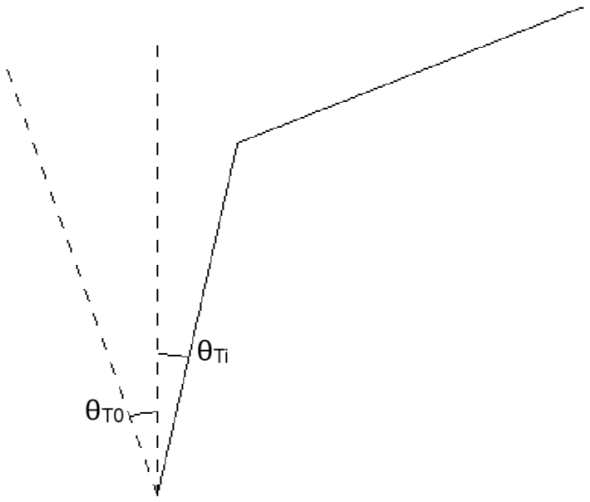

θTi $= \tan^{-1}(X_3/Y_3)$

θp $= \theta Ti - \theta To$; only needed is tube is off from vertical at test start.

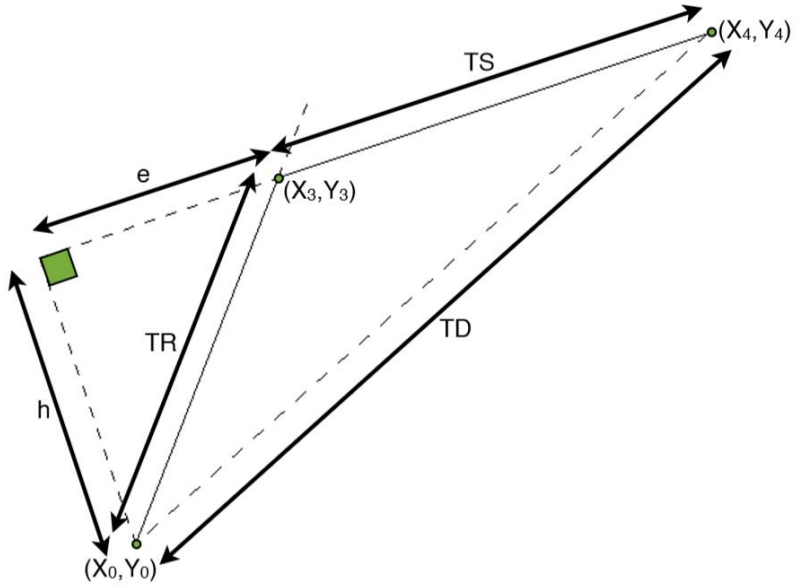

TD^2	$=h^2+(TS+e)^2=h^2+TS^2+2TSe+e^2$
TR^2	$=h^2+e^2$
TD^2-TR^2	$=TS^2+2TSe$
e	$=[TD^2-TR^2-TS^2]/[2TS]$
h	$SQRT(TR^2-e^2)$

As conclusion, all needed parameters (h, θ) are obtained to plot moment rotation curves from test readings.